

On differential operators for scalar-scaffolded gluons

Jin Dong,^b Yong-Xiang Su^c and Dongyu Yang^{a,d,e}

^a*School of Fundamental Physics and Mathematical Sciences, Hangzhou Institute for Advanced Study, UCAS, Hangzhou 310024, China*

^b*Max-Planck-Institut für Physik, Werner-Heisenberg-Institut, Boltzmannstr. 8, 85748 Garching bei München, Germany*

^c*School of Physical Sciences, University of Science and Technology of China, Hefei, Anhui 230026, China*

^d*Institute of Theoretical Physics, Chinese Academy of Sciences, Beijing 100190, China*

^e*School of Physical Sciences, University of Chinese Academy of Sciences, Beijing 100049, China*

E-mail: jindong@mpp.mpg.de, anonym@mail.ustc.edu.cn,

yangdongyu24@mails.ucas.ac.cn

ABSTRACT: Recently, based on the curve-integral formulation for stringy $\text{Tr}\phi^3$ amplitudes, a combinatorial formulation for Yang-Mills amplitudes has been proposed which describes gluons using pairs of scalars and produces the n -gluon amplitude from simple kinematical shift of stringy $\text{Tr}\phi^3$ amplitudes with $2n$ scalars. It has revealed a variety of new properties and structures even for tree-level gluon amplitudes such as hidden zeros and splits, and in this note we provide another example: we study differential operators acting on Yang-Mills amplitudes with respect to $2n$ -scalar kinematic variables, which convert such scalar-scaffolded gluons into scalars. In particular, we find $(n-1)$ -fold differential operators (using $2n$ -scalar variables) that turn the n -gluon amplitude into a single planar ϕ^3 diagram; we then generalize such operators to those that convert n gluons to mixed amplitudes with r scalars and $n-r$ gluons (the latter can be viewed as insertions on ϕ^3 diagrams). We also show that the number of linearly independent mixed amplitudes with r scalars and $n-r$ gluons is given by the number of ϕ^3 diagrams, the Catalan number \mathcal{C}_{r-2} , which can be viewed as a generalization of the “uniqueness” theorem of gluon amplitudes (with $r=0$). Finally, our construction leads to a planar version of the universal expansion of Yang-Mills amplitudes into a sum of gauge-invariant prefactors built from nested commutators, each accompanied by an mixed amplitude in the natural basis. This formulation significantly reduces the redundancy present in the original expansion.

Contents

| | | |
|----------|---|-----------|
| 1 | Introduction | 1 |
| 2 | Review | 3 |
| 2.1 | Scaffolded gluon amplitudes | 3 |
| 2.2 | Transmuted operators | 7 |
| 2.3 | Universal expansion | 9 |
| 3 | Scalar Cubic Diagram from Derivatives | 10 |
| 3.1 | General rules and examples | 11 |
| 3.2 | Proof of the rules by factorization | 16 |
| 4 | Gluon Insertions and Minimal Basis | 20 |
| 5 | Gluon Insertions from Derivative | 24 |
| 6 | The Planar Universal Expansion | 28 |
| 7 | Conclusions and Outlook | 31 |
| A | Details of Minimal Basis for Mixed Amplitudes | 32 |
| A.1 | 6-point 2-gluon examples | 32 |
| A.2 | Proof | 32 |
| B | Details for 5-point planar universal expansion | 37 |
| | Bibliography | 38 |

1 Introduction

Over the past few decades, significant progress has been made in uncovering the hidden structures of scattering amplitudes in quantum field theory. Perhaps one of the most celebrated developments is the Bern-Carrasco-Johansson (BCJ) double copy relation [1, 2], which establishes a deep connection between gauge and gravity amplitudes. The Cachazo-He-Yuan (CHY) formula [3–5] has further unified a broad class of theories into a common foundation, enabling explicit constructions of Yang-Mills (YM) amplitudes and their gravitational double copies [6–9] (see also [10–15] for recent advances). Concretely, in the Del Duca-Dixon-Maltoni (DDM) half-ladder basis [16], the YM amplitude can be expressed as a sum over $(n - 2)!$ bi-adjoint ϕ^3 amplitudes accompanied by the corresponding BCJ numerators. The CHY representation makes this structure manifest and provides a powerful tool for computing explicit BCJ numerators. However, their naive construction depends

on a reference ordering, which breaks crossing symmetry and complicates the computation (one solution is to restore the crossing symmetry as in [11], which is equivalent to averaging over all reference orderings). On the other hand, if one is only concerned with color-ordered YM amplitudes, the asymptotic complexity is expected to grow exponentially, since the number of ordered cubic diagrams is given by the Catalan number.

A recent breakthrough on reformulation of scattering amplitudes for $\text{Tr } \phi^3$ to all orders in the 't Hooft topological expansion, known as the curve integral has been introduced in [17, 18]. This framework has also been generalized to the scattering of pions and gluons in the planar limit in a series of works [19–21] revealing hidden zeros of corresponding amplitudes as well as novel properties such as factorization near zeros and special splitting behaviors [19, 22–25] (see also for related results [26–39]). With this approach, tree-level YM amplitudes (and even loop integrands) admit a novel representation in terms of scalar-scaffolding variables. These variables trivialize the constraint of momentum conservation and provide a simple, unique representation of YM amplitudes, while key properties such as gauge invariance and factorization at simple poles are presented in a different way. The above development suggests that there might be a better approach to the YM amplitudes, of which the complexity grows exponentially.

On the other hand, in the traditional representation, differential operators involving polarization vectors and momenta relate YM amplitudes to both $\text{YM}+\phi^3$ mixed amplitudes [40] and pure scalar ones by systematically lowering the spin of external states. The products of these operators act locally on the kinematic data and preserve essential structural properties, *i.e.* momentum conservation and gauge invariance, making them an efficient tool for navigating between theories of different spin. Nevertheless, the analogous story for scalar-scaffolded amplitudes remains largely unexplored (however, see [41] for a related paper). Since the gluon, scalar, and mixed amplitudes are all simple and unique objects in these variables, it is natural to expect a straightforward connection through differential operators. Establishing such relations would not only generalize the traditional transmutation program into the new formalism, but also shed light on hidden structures of YM amplitudes and potentially offer a more efficient route for generating mixed amplitudes within the planar framework.

In this paper, we begin to address the above questions through the following steps. We first develop a systematic method for deriving differential operators that extract single scalar cubic diagrams from the scalar-scaffolded YM amplitude. Building on this construction, we then investigate generalizations of these differential operators, showing that while in some cases they naturally lead to insertions of gluons, in other cases the naive generalization fails. We also demonstrate that the number of linearly independent mixed amplitudes of r scalars and $n - r$ gluons is counted by the Catalan number \mathcal{C}_{r-2} . Altogether, these developments lead to a planar version of the universal expansion of Yang-Mills amplitudes, expressed as a sum of gauge-invariant prefactors built from nested commutators, each paired with a mixed amplitude in the natural basis. This result offers a streamlined perspective that greatly reduces the redundancy of the traditional expansion.

This paper is organized as follow: In section 2, we review the scalar-scaffolded gluon amplitudes and transmutation operators, as well as the universal expansion of YM am-

plitudes into YM+ ϕ^3 mixed amplitudes and pure scalar ones. In section 3, we present a systematic algorithm for obtaining single ϕ^3 diagram by operating a sequence of derivatives acting on the scalar-scaffolded YM amplitude and provide proofs of our rules for certain cases using factorization. Based on the insight from planarity, we show in section 4 that the number of independent mixed amplitudes is determined only by the number of scalars within, counted by Catalan numbers. Then in section 5, we discuss the feasibility that whether similar differential operators could be used to derived mixed amplitudes within the natural planar basis. Finally section 6 reorganizes the conventional form of universal expansion into such basis.

2 Review

2.1 Scaffolded gluon amplitudes

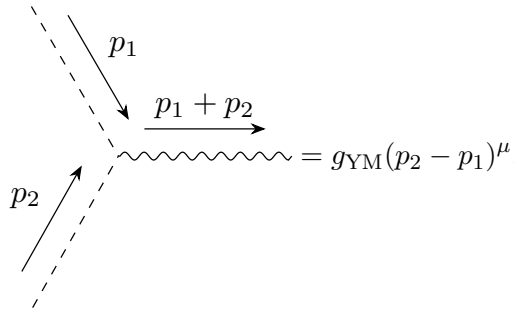
In this section, we give a lightning review of scalar-scaffolded gluon amplitudes[19, 20, 42]¹. To begin with, we define the planar variables

$$X_{i,j} \equiv (p_i + p_{i+1} + \cdots + p_{j-1})^2. \quad (2.1)$$

By definition, we have $X_{i,j} = X_{j,i}$ and $X_{i,i} = X_{i,i+1} = 0$ for massless particles. The usual Mandelstam variables are related to these invariants via the ABHY [47] conditions

$$c_{i,j} \equiv -2p_i \cdot p_j = X_{i,j} + X_{i+1,j+1} - X_{i,j+1} - X_{i+1,j}. \quad (2.2)$$

For an n -point gluon amplitude, we consider expanding the external gluon legs into double scalar legs with the following Feynman vertex:



$$= g_{\text{YM}}(p_2 - p_1)^\mu, \quad (2.3)$$

where g_{YM} is the gluon coupling constant. In this setup, each pair of YMS scalars is scaffolded into a gluon. To extract the n -point YM amplitude, one must take the intermediate gluons on-shell in the $2n$ -point (*i.e.* n -pair) amplitude, evaluated on the following scaffolding residues:

$$X_{1,3} = X_{3,5} = X_{5,7} = \cdots = X_{2n-1,1} = 0. \quad (2.4)$$

Such operation can be depicted on a surface with $2n$ -punctures on the edge. Taking the scaffolding of a scalar amplitude is equivalent pictorially as pinching the $2i - 1$ -th and $2i$ -th vertex into one and collapse the $2n$ -gon into an n -gon (see figure 1).

¹Similar ideas were also briefly discussed in previous works; see for example [43–46].

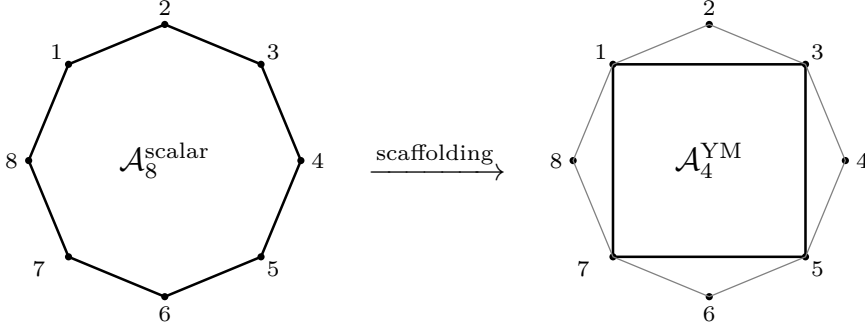


Figure 1: Scaffolding from 8-scalar amplitude $\mathcal{A}_8^{\text{scalar}}(1, 2, 3, 4, 5, 6, 7, 8)$ to 4-gluon amplitude $\mathcal{A}_4^{\text{YM}}(1, 3, 5, 7)$.

It is straightforward to verify that the kinematic data, specifically the gluon polarizations and momenta, are fully captured by the scaffolded planar variables. For example, for an tree-level n -point Yang-Mills amplitude, there are $n(n-3)/2$ independent scalar products $k_i \cdot k_j$, $n(n-1)/2$ polarization contractions $\epsilon_i \cdot \epsilon_j$, and $n(n-1) - n$ mixed terms $\epsilon_i \cdot p_j$, giving a total of $2n(n-2)$ independent kinematic variables. On the other hand, for a $2n$ -point scalar amplitude, the number of independent kinematic variables is $2n(2n-3)/2 - n = 2n(n-2)$, which precisely matches the count for the gluon case.

To be precise, the momentum of the i -th gluon k_i^μ is given by

$$k_i^\mu = (p_{2i-1} + p_{2i})^\mu. \quad (2.5)$$

The polarization, on the other hand, contains a free parameter λ , which is associated with the gauge redundancy.

$$\epsilon_i^\mu = (1 - \lambda)p_{2i-1}^\mu - \lambda p_{2i}^\mu, \quad (2.6)$$

which one can verify it satisfying the transversality condition $\epsilon_i \cdot k_i = 0$ and manifesting a generalized ‘‘circular polarizations’’ $\epsilon_i \cdot \epsilon_i = 0$.

A benefit for the scaffolding language is that it can manifest the gauge invariance and multi-linearity in a unifying way. For the i -th gluon, its gauge transformation reads

$$\epsilon_i^\mu \rightarrow \epsilon_i^\mu + \alpha k_i^\mu \quad \forall \alpha \in \mathbb{C}, \quad (2.7)$$

which can be translated into (with $\lambda = \frac{1}{2}$)

$$X_{2i,j} \rightarrow X_{2i,j} + \alpha(X_{2i+1,j} - X_{2i-1,j}). \quad (2.8)$$

Thus the gauge invariance condition for the i -th gluon becomes

$$\mathcal{A}_n^{\text{YM}}[X_{2i,j} + \alpha(X_{2i+1,j} - X_{2i-1,j})] - \mathcal{A}_n^{\text{YM}}[X_{2i,j}] = 0. \quad (2.9)$$

For the multi-linearity, consider

$$\epsilon_i^\mu \rightarrow \epsilon_i^\mu + \beta \epsilon_i^\mu \quad \forall \beta \in \mathbb{C}, \quad (2.10)$$

which is given by

$$X_{2i,j} \rightarrow X_{2i,j} + \frac{\beta}{2}(X_{2i,j} - X_{2i-1,j}) + \frac{\beta}{2}(X_{2i,j} - X_{2i+1,j}). \quad (2.11)$$

This gives us the scaffolding form of multi-linearity condition on i -th gluon

$$\mathcal{A}_n^{\text{YM}} \left[X_{2i,j} \rightarrow X_{2i,j} + \frac{\beta}{2}(X_{2i,j} - X_{2i-1,j}) + \frac{\beta}{2}(X_{2i,j} - X_{2i+1,j}) \right] - \mathcal{A}_n^{\text{YM}}[X_{2i,j}] = \beta \mathcal{A}_n^{\text{YM}}[X_{2i,j}]. \quad (2.12)$$

Combine equations (2.9) and (2.12), we obtain a compact formula

$$\mathcal{A}_n^{\text{YM}} \left[X_{2i,j} \rightarrow X_{2i,j} + \alpha(X_{2i+1,j} - X_{2i-1,j}) + \frac{\beta}{2}(X_{2i,j} - X_{2i-1,j}) + \frac{\beta}{2}(X_{2i,j} - X_{2i+1,j}) \right] - \mathcal{A}_n^{\text{YM}}[X_{2i,j}] = \beta \mathcal{A}_n^{\text{YM}}[X_{2i,j}]. \quad (2.13)$$

Picking $\alpha = \pm \frac{\beta}{2}$, we have:

$$\mathcal{A}_n^{\text{YM}}[X_{2i,j} \rightarrow X_{2i,j} + \beta(X_{2i,j} - X_{2i-1,j})] - \mathcal{A}_n^{\text{YM}} = \beta \mathcal{A}_n^{\text{YM}}, \quad (2.14)$$

$$\mathcal{A}_n^{\text{YM}}[X_{2i,j} \rightarrow X_{2i,j} + \beta(X_{2i,j} - X_{2i+1,j})] - \mathcal{A}_n^{\text{YM}} = \beta \mathcal{A}_n^{\text{YM}}. \quad (2.15)$$

This is equivalent to the following:

$$\mathcal{A}_n^{\text{YM}} = \sum_{j \neq i-1, i, i+1} (X_{2i,j} - X_{2i-1,j}) \frac{\partial}{\partial X_{2i,j}} \mathcal{A}_n^{\text{YM}}, \quad (2.16)$$

$$\mathcal{A}_n^{\text{YM}} = \sum_{j \neq i-1, i, i+1} (X_{2i,j} - X_{2i+1,j}) \frac{\partial}{\partial X_{2i,j}} \mathcal{A}_n^{\text{YM}}, \quad (2.17)$$

where we have used the fact that at each given term, even label $2i$ appears as a subscript in at most one X . Note that one of the above conditions can be replaced by:

$$(2.16) - (2.17) = \sum_{j \neq i-1, i, i+1} (X_{2i+1,j} - X_{2i-1,j}) \frac{\partial}{\partial X_{2i,j}} \mathcal{A}_n^{\text{YM}} = 0. \quad (2.18)$$

The factorization of the gluon amplitude also manifests in our scalar-scaffolded language. Denote $X_{a,b}$ for both a, b odd as the gluon propagator we are considering, the residue of the gluon amplitude at $X_{a,b} = 0$ is given by the linear combination of planar variables and derivative of partial amplitudes:

$$\text{Res}_{X_{a,b}=0} \mathcal{A}_n^{\text{YM}} = \sum_{j,J} (X_{j,J} - X_{a,j} - X_{b,J}) \frac{\partial}{\partial X_{x,j}} \mathcal{A}_L \frac{\partial}{\partial X_{x',J}} \mathcal{A}_R, \quad (2.19)$$

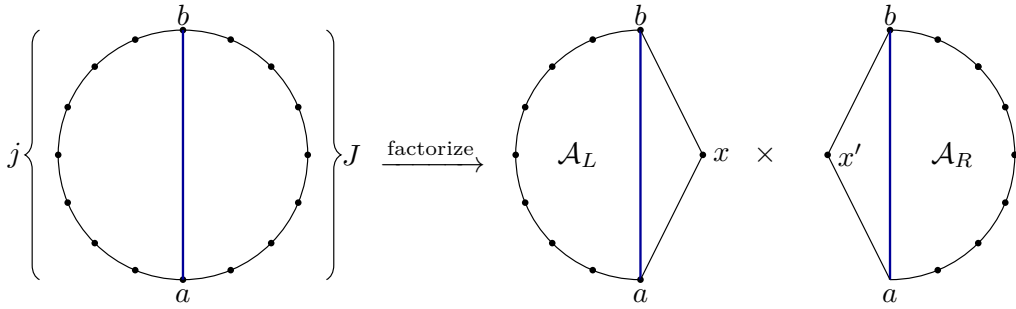


Figure 2: $\mathcal{A}_n^{\text{YM}}$ factorizes on $X_{a,b}$, forming a pair of sub-amplitudes \mathcal{A}_L and \mathcal{A}_R .

where the summation is over all $j = a + 1, \dots, b - 1$ and $J = b + 1, \dots, a - 1$, and punctures x and x' are axillary points to ensure that the partial amplitudes $\mathcal{A}_L(a, \dots, b, x)$ and $\mathcal{A}_R(b, \dots, x')$ are also formulated by scaffolded scalars (see figure 2).

Given that one can label the vertices either clockwise or counterclockwise, it is natural to expect a greater symmetry in the labels a and b appearing in the prefactor. In fact, there are three additional equivalent ways to express the factorization, differing only in the subscripts a and b of the prefactor. Let us list them explicitly:

$$\text{Res}_{X_{a,b}=0} \mathcal{A}_n^{\text{YM}} = \sum_{j,J} (X_{j,J} - X_{b,j} - X_{a,J}) \frac{\partial}{\partial X_{x,j}} \mathcal{A}_L \frac{\partial}{\partial X_{x',J}} \mathcal{A}_R, \quad (2.20)$$

$$\text{Res}_{X_{a,b}=0} \mathcal{A}_n^{\text{YM}} = \sum_{j,J} (X_{j,J} - X_{a,j} - X_{a,J}) \frac{\partial}{\partial X_{x,j}} \mathcal{A}_L \frac{\partial}{\partial X_{x',J}} \mathcal{A}_R, \quad (2.21)$$

$$\text{Res}_{X_{a,b}=0} \mathcal{A}_n^{\text{YM}} = \sum_{j,J} (X_{j,J} - X_{b,j} - X_{b,J}) \frac{\partial}{\partial X_{x,j}} \mathcal{A}_L \frac{\partial}{\partial X_{x',J}} \mathcal{A}_R. \quad (2.22)$$

It is easy to verify that the difference between the right hand sides of any two of these expressions vanishes. For example, the difference between (2.19) and (2.21) is given by

$$\sum_j \frac{\partial}{\partial X_{x,j}} \mathcal{A}_L \sum_J (X_{a,J} - X_{b,J}) \frac{\partial}{\partial X_{x',J}} \mathcal{A}_R, \quad (2.23)$$

where we have

$$(X_{a,J} - X_{b,J}) \frac{\partial}{\partial X_{x',J}} \mathcal{A}_R = 0. \quad (2.24)$$

Here we have used the fact that in \mathcal{A}_R we have labeled $x' - 1 = a$ and $x' + 1 = b$, therefore the expression (2.24) matches exactly the identity (2.18) when applied to \mathcal{A}_R .

To conclude this section, we present the translation between the usual Lorentz products and the scalar-scaffolded planar variables [20]. For simplicity, we set $\lambda = 1$, which does not

affect the gauge-invariant amplitude:

$$\begin{aligned}
2\epsilon_i \cdot \epsilon_j &= X_{2i,2j-1} + X_{2i-1,2j} - X_{2i-1,2j-1} - X_{2i,2j}, \\
2\epsilon_i \cdot k_j &= X_{2i,2j+1} - X_{2i,2j-1} + X_{2i-1,2j-1} - X_{2i-1,2j+1}, \\
2k_i \cdot k_j &= X_{2i-1,2j+1} + X_{2i+1,2j-1} - X_{2i-1,2j-1} - X_{2i+1,2j+1}.
\end{aligned} \tag{2.25}$$

For example, the explicit expression for $n = 3$ reads:

$$\mathcal{A}_3^{\text{YM}} = -4(k_2 \cdot \epsilon_3 \epsilon_1 \cdot \epsilon_2 + k_1 \cdot \epsilon_2 \epsilon_1 \cdot \epsilon_3 + k_2 \cdot \epsilon_1 \epsilon_2 \cdot \epsilon_3). \tag{2.26}$$

Substituting equations (2.25) the amplitude becomes

$$\mathcal{A}_3^{\text{YM}} = -X_{1,4}X_{2,5} + X_{1,4}X_{2,6} - X_{1,4}X_{3,6} + X_{2,4}X_{3,6} - X_{2,5}X_{3,6} + X_{2,5}X_{4,6}. \tag{2.27}$$

For explicit results up to $n = 7$, see [42]. We also employ the $2n$ scalar-scaffolded variables to describe the mixed amplitudes of gluons and colored ϕ^3 scalars [48]. Note that an even label $2i$ appears in the subscripts of the X 's only if particle i is a gluon. For example,

$$\mathcal{A}_3^{\text{YM}+\phi^3}(\{2\}|1,3) = -2k_1 \cdot \epsilon_2 = X_{1,4}, \tag{2.28}$$

where we consider the three-point mixed amplitude with particle 2 being a gluon; hence the even label 4 appears.

2.2 Transmuted operators

An elegant way to relate scattering amplitudes across different theories is through the use of specific differential operators [40, 49]. For our purposes, we focus on those operators that transform gluons into bi-adjoint scalars. To be more explicitly, these operators are defined by a set of derivatives on kinematic variables:

$$\mathcal{T}_{i,j} := \partial_{\epsilon_i \cdot \epsilon_j}, \tag{2.29}$$

$$\mathcal{T}_{i,j,k} := \partial_{p_i \cdot \epsilon_j} - \partial_{p_k \cdot \epsilon_j}. \tag{2.30}$$

Crucially, any well-defined combination of these operators must preserve both momentum conservation and gauge invariance. To incorporate these constraints we define a the total momentum operator for momentum conservation

$$\mathcal{P}_v := \sum_{i=1}^n p_i \cdot v, \tag{2.31}$$

and the Ward identity operator for gauge invariance

$$\mathcal{W}_i := \sum_v p_i \cdot v \partial_{v \cdot \epsilon_i}, \tag{2.32}$$

where i denotes external legs and v labels any momentum or polarization vector. Any gauge invariant and momentum conserving amplitude A is annihilated by these operators, that is to say

$$\mathcal{P}_v \cdot A = \mathcal{W}_i \cdot A = 0. \quad (2.33)$$

One can check that both length-2 and length-3 transmuted operators satisfy momentum conservation

$$[\mathcal{P}_v, \mathcal{T}_{i,j}] \cdot A = [\mathcal{P}_v, \mathcal{T}_{i,j,k}] \cdot A = 0. \quad (2.34)$$

However, only the length-2 transmuted operator seems to obey gauge invariance such that

$$[\mathcal{W}_l, \mathcal{T}_{i,j}] \cdot A = 0, \quad (2.35)$$

while as an exception, the commutator of $\mathcal{T}_{i,j,k}$ with \mathcal{W}_l reveals a non-trivial result

$$[\mathcal{W}_l, \mathcal{T}_{i,j,k}] \cdot A = \delta_{kl} \mathcal{T}_{j,k} \cdot A - \delta_{il} \mathcal{T}_{i,j} \cdot A. \quad (2.36)$$

We emphasize that even as $\mathcal{T}_{i,j,k}$ does not manifest gauge invariance intrinsically, it can still be effectively gauge invariant when combined with enough supplemental transmuted operators. For example, the commutator of \mathcal{W}_l with the product $\mathcal{T}_{i,k} \mathcal{T}_{i,j,k}$ gives

$$[\mathcal{T}_{i,k} \cdot \mathcal{T}_{i,j,k}, \mathcal{W}_l] \cdot A = \delta_{il} \mathcal{T}_{i,k} \cdot \mathcal{T}_{i,j} \cdot A - \delta_{k,l} \mathcal{T}_{i,k} \cdot \mathcal{T}_{j,k} \cdot A = 0, \quad (2.37)$$

where at the second equal sign we have used the condition that the amplitude A is multi-linear in polarizations ϵ_i and ϵ_k , leading it vanishing after being twice interacted by transmuted operators $\mathcal{T}_{i,k} \cdot \mathcal{T}_{i,j}$ and $\mathcal{T}_{i,k} \cdot \mathcal{T}_{j,k}$.

Applied in various combinations, the transmutation operators form an interlocking web of scattering amplitudes relations across a wide range of theories. For single trace operators defined by a sequence of transmuted operators in an ordered list α

$$\mathcal{T}[\alpha] := \mathcal{T}_{\alpha_1, \alpha_n} \cdot \prod_{i=2}^{n-1} \mathcal{T}_{\alpha_{i-1}, \alpha_i, \alpha_n}, \quad (2.38)$$

they can transform an amplitude of gluons into the one of gluons mixed with bi-adjoint scalars

$$\mathcal{T}[\alpha] \mathcal{A}_n^{\text{YM}} = \mathcal{A}_n^{\text{YM}+\phi^3}(\{\bar{\alpha}\}|\alpha), \quad (2.39)$$

in which $\{\bar{\alpha}\}$ denotes remaining gluons.

Given the success of these operators, it is natural to ask whether analogous operators exist in the scaffolded variables acting directly on amplitudes expressed in this form. Since the relation between these variables and the usual Lorentz products was discussed in [20], one can in principle obtain an exact map using the chain rule. However, as we will see later, there exists a more natural choice that leads to a better basis.

2.3 Universal expansion

The expansion of Yang-Mills amplitudes on Yang-Mills-scalar amplitudes was originally proposed in [7, 8, 50] by studying the CHY representation of Yang-Mills and Yang-Mills scalar amplitudes, and later realized as a consequence of basic principles *i.e.* power counting, locality and gauge invariance [51]. The explicit formula is given by

$$\mathcal{A}_n^{\text{YM}} = \sum_{m, \alpha \in S_m} (-1)^m \epsilon_1 \cdot f_{\alpha_1} \cdot f_{\alpha_2} \cdots f_{\alpha_m} \cdot \epsilon_n \mathcal{A}_n^{\text{YM}+\phi^3}(\{\bar{\alpha}\}|1, \alpha, n), \quad (2.40)$$

Note that both particle 1 and n are special and the sum is over all *ordered subsets* of $\{2, 3, \dots, n-1\}$ denoted by α (with $|\alpha| = m$ for $m = 0, 1, \dots, n-2$), and $\{\bar{\alpha}\}$ denotes the complementary (unordered) set with $n-2-m$ labels. For particles $2, \dots, (n-1)$, the gauge invariance is manifest in (2.40), since we are summing over prefactors that contain $f_i^{\mu\nu} \equiv k_i^\mu \epsilon_i^\nu - \epsilon_i^\mu k_i^\nu$ multiplied with a mixed amplitude involving gluons $\bar{\alpha}$ and doubly ordered ϕ^3 scalars, where the second ordering is labeled by $(1, \alpha, n)$. The gauge invariance of particle 1(or n), however, is not obvious. Actually, according to [52], if we express the Yang-Mills amplitudes with a local form, as is the case in (2.40), it is only possible to manifest the gauge invariance of $(n-2)$ particles. Furthermore, as proven in [51], requiring the gauge invariance of $(n-2)$ particles already spits out the prefactors, yet one can not confirm that the gauge invariant block accompanied with the prefactor is indeed a YMS amplitude. The next step is to use the gauge invariance of another particle say the first particle, which uniquely fixes the Yang-Mills amplitudes, as well as its expansion (2.40).

As to present more concretely, we provide a few examples for this expansion. For $n = 3$, the expansion is quite trivial,

$$\mathcal{A}_3^{\text{YM}} = \epsilon_1 \cdot \epsilon_3 \mathcal{A}_3^{\text{YM}+\phi^3}(\{2\}|13) - \epsilon_1 \cdot f_2 \cdot \epsilon_3 \mathcal{A}_3^{\text{YM}+\phi^3}(\emptyset|123). \quad (2.41)$$

For $n = 4$, we have 3 different kinds of terms, each corresponds to $m = 0, 1, 2$:

$$\begin{aligned} \mathcal{A}_4^{\text{YM}} = & \epsilon_1 \cdot \epsilon_4 \mathcal{A}_4^{\text{YM}+\phi^3}(\{2, 3\}|1, 4) - \epsilon_1 \cdot f_2 \cdot \epsilon_4 \mathcal{A}_4^{\text{YM}+\phi^3}(\{3\}|1, 2, 4) - \epsilon_1 \cdot f_3 \cdot \epsilon_4 \mathcal{A}_4^{\text{YM}+\phi^3}(\{2\}|1, 3, 4) \\ & + \epsilon_1 \cdot f_2 \cdot f_3 \cdot \epsilon_4 \mathcal{A}_4^{\text{YM}+\phi^3}(\emptyset|1, 2, 3, 4) + \epsilon_1 \cdot f_3 \cdot f_2 \cdot \epsilon_4 \mathcal{A}_4^{\text{YM}+\phi^3}(\emptyset|1, 3, 2, 4), \end{aligned} \quad (2.42)$$

We also provide explicit expression for 5-point expansion in Appendix B.

We remark that the number of terms in this expansion is

$$\sum_{m=0}^{n-2} m! \binom{n-2}{m}, \quad (2.43)$$

which equals to 2, 5, 16, 65, 326, 1957 for $n = 3, 4, 5, 6, 7, 8$, and asymptotically behaves as $(n-2)!e$ for large n (see [OEIS A000522](#)). It is then reasonable to ask whether there exists a planar analogue of this expansion in the scaffolded variables that respects the Catalan-number counting.

3 Scalar Cubic Diagram from Derivatives

In this section, we investigate differential operators that generate single cubic diagrams. Note that the derivatives involving conventional variables built from Lorentz contractions of ϵ and p are highly restrictive under momentum conservation [40]. In contrast, the planar variables automatically encode momentum conservation, admit derivatives free of such constraints.

The power counting of YM amplitudes is given by X^2 for any n . To extract ϕ^3 scalar diagrams (amplitudes) that scale as $1/X^{n-3}$, one needs to act with derivatives involving $n-1$ distinct planar variables $X_{i,j}$. Such derivatives are not expected to involve $X_{o,o}$, since these variables could appear in the denominator. Moreover, they are constrained by multilinearity: in each term, every even label $2i$ (with $i = 1, 2, \dots, n$) appears as a subscript in at most one X . Consequently, we have

$$\frac{\partial^2}{\partial X_{2a,b} \partial X_{2a,b'}} \mathcal{A}_n^{\text{YM}} = 0. \quad (3.1)$$

And we expect the relevant derivatives to involve $n-1$ variables: one of the form $X_{e,e}$ and $n-2$ of the form $X_{e,o}$, *i.e.*

$$\mathcal{D}_{(2a',2b'),(2a_1,2b_1-1),\dots,(2a_{n-2},2b_{n-2}-1)} \equiv \frac{\partial^{n-1}}{\partial X_{2a',2b'} \partial X_{2a_1,2b_1-1} \dots \partial X_{2a_{n-2},2b_{n-2}-1}}. \quad (3.2)$$

It is natural to fix $2a'$ and $2b'$ to be adjacent even integers²; without loss of generality, we choose $(2a', 2b') = (2, 2n)$. It is straightforward to see from (2.27) that for 3-point we have $\mathcal{D}_{(2,6)(1,4)} \mathcal{A}_3^{\text{YM}} = 1$. Experimentally, for $n = 4$ we find³:

$$\mathcal{D}_{(2,8)(1,4)(1,6)} \mathcal{A}_4^{\text{YM}} = \frac{1}{X_{1,5}}, \quad \mathcal{D}_{(2,8)(1,4)(3,6)} \mathcal{A}_4^{\text{YM}} = \frac{1}{X_{3,7}}, \quad (3.3)$$

and similarly:

$$\mathcal{D}_{(2,8)(4,7)(1,6)} \mathcal{A}_4^{\text{YM}} = \frac{1}{X_{3,7}}, \quad \mathcal{D}_{(2,8)(4,7)(3,6)} \mathcal{A}_4^{\text{YM}} = -\frac{1}{X_{3,7}}. \quad (3.4)$$

For $n = 5$, we have:

$$\mathcal{D}_{(2,10)(1,4)(1,6)(1,8)} \mathcal{A}_5^{\text{YM}} = \frac{1}{X_{1,5} X_{1,7}}, \quad \mathcal{D}_{(2,10)(1,4)(3,6)(3,8)} \mathcal{A}_5^{\text{YM}} = \frac{1}{X_{3,7} X_{3,9}}. \quad (3.5)$$

Clearly these are exactly the derivatives that produce the desired single cubic scalar diagrams. Of course there are operators that resulting in sum of cubic diagrams or 0, for

²In fact, using the relation between scaffolding variables and the usual Lorentz products [20], it is straightforward to show that $\partial_{X_{2a',2b'}} \sim \partial_{\epsilon_{a'} \cdot \epsilon_{b'}}$.

³The overall sign of the YM amplitude is fixed so that the ray-like diagram, where all points are connected to vertex-1, obtained from the general rules (described in the next subsection) corresponds to a positive sign. Consequently, all other diagrams will also carry a positive sign.

examples:

$$\mathcal{D}_{(2,10)(1,4)(6,9)(5,8)}\mathcal{A}_5^{\text{YM}} = -\frac{1}{X_{1,5}X_{5,9}} - \frac{1}{X_{3,9}X_{5,9}}, \quad \mathcal{D}_{(2,10)(1,4)(1,6)(3,8)}\mathcal{A}_5^{\text{YM}} = 0. \quad (3.6)$$

While it would be interesting to study the results of all possible inequivalent derivatives, for our purposes, it is particularly useful to first apply $\partial/\partial X_{1,4}$ (or $\partial/\partial X_{1,n-2}$) in addition to $\partial/\partial X_{2,2n}$. This choice ensures that the remaining $X_{e,o}$ derivatives correspond one-to-one with propagators $X_{o',e}$ (with $o' = e \pm 1$) in the resulting diagram, according to our rules. In the following subsections, we present the general rules and provide a proof for certain cases based on factorization.

3.1 General rules and examples

For a given cubic diagram, we denote its propagators $X_{i,j}$ by (i, j) , where $1 \leq i < j \leq 2n-1$ and both i and j are odd integers. In this way, the diagram is represented by a sequence of diagonals $(i_1, j_1), \dots, (i_{n-3}, j_{n-3})$, with each (i, j) corresponding to a diagonal connecting vertices i and j .

On the other hand, we denote the differential operators $\partial/\partial X_{a,b}$ by $[a, b]$, where $1 \leq a < b \leq 2n$. Thus the sequence of operators is written as $[a_1, b_1], \dots, [a_{n-3}, b_{n-3}]$, with $[2, 2n]$ and $[1, 4]$ omitted for brevity. Note that since we always perform these two derivatives first, the subsequent steps will never involve operators like $[2, a]$, $[4, b]$, or $[2n, c]$. In particular, vertices 1 and 3 play a special role in the construction.

By definition, they satisfy the symmetries $(i, j) = (j, i)$ and $[a, b] = [b, a]$. However, in certain cases, propagators may intentionally be written as (j, i) with $i < j$ in order to apply specific rules. The correspondence between differential operators and single cubic diagrams is summarized below:

1. For a given single cubic diagrams, reorganize the sequence of propagators $(i_1, j_1)(i_2, j_2)\dots(i_{n-3}, j_{n-3})$ until it satisfies: if a propagator (i_t, j_t) does not contain vertex-1 or 3 and $i_t \neq i_{t-1}$, then $i_t = j_{t-1}$ ($2 \leq t \leq n-3$). In other words, the sequence should be made as consecutively connected as possible. Additionally, the sequence must start from vertex-1 or 3, since the subregion $\{1, 2, 3, 2n\}$ must be triangulated, implying that at least one diagonal must be connected to vertex-1 or 3. For some cases where cycles appear (note that only cycles containing vertex-1 or 3 are considered), if vertex-1 is in the cycle, then the cycle should be written in a clockwise order in the sequence, otherwise the cycle should be written in a counterclockwise order. For examples, the 6-point zigzag and cycle diagrams (see figure 5) $1/X_{1,5}X_{5,11}X_{7,11}$, $1/X_{3,7}X_{3,11}X_{7,11}$ is now labeled by $(1, 5)(5, 11)(11, 7)$ and $(3, 11)(11, 7)(7, 3)$, respectively.
2. Next, we assign an operator to each propagator connected to vertex-1 or 3, according

to the following rule:

$$\begin{aligned}
(1, j) &\longleftrightarrow [1, j + 1], \\
(3, j) &\longleftrightarrow [3, j - 1], \\
(i, 1) &\longleftrightarrow [i + 1, 1], \\
(i, 3) &\longleftrightarrow [i - 1, 3].
\end{aligned} \tag{3.7}$$

For the 6-point zigzag diagram we mentioned above, we fix one derivative $(1, 5) \leftrightarrow [1, 6]$; and for the cycle we fix two $(3, 11) \leftrightarrow [3, 10]$, $(11, 3) \leftrightarrow [10, 3]$.

3. The remaining differential operators are determined recursively as follows:

$$\begin{aligned}
\cdots (1, j)(i', j') \cdots &\longleftrightarrow \cdots [1, j + 1][i', j' - 1] \cdots \\
\cdots (i, 1)(i', j') \cdots &\longleftrightarrow \cdots [i + 1, 1][i', j' - 1] \cdots
\end{aligned} \quad (j' \neq 1, 3, i' \neq 1), \tag{3.8}$$

$$\begin{aligned}
\cdots (3, j)(i', j') \cdots &\longleftrightarrow \cdots [3, j - 1][i', j' + 1] \cdots \\
\cdots (i, 3)(i', j') \cdots &\longleftrightarrow \cdots [i - 1, 3][i', j' + 1] \cdots
\end{aligned} \quad (j' \neq 1, 3, i' \neq 3), \tag{3.9}$$

$$\cdots (i, j)(i', j') \cdots \longleftrightarrow \begin{cases} \cdots [i, j \pm 1][i', j \pm 1] \cdots & \text{if } i = i', \\ \cdots [i, j \pm 1][i', j \mp 1] \cdots & \text{otherwise.} \end{cases} \tag{3.10}$$

Moving back to the previous examples, for zigzag we have $(1, 5)(5, 11) \leftrightarrow [1, 6][5, 10]$ and then $(1, 5)(5, 11)(11, 7) \leftrightarrow [1, 6][5, 10][11, 8]$; similarly for cycle we conclude $(3, 11)(11, 7)(7, 3) \leftrightarrow [3, 10][11, 8][6, 3]$.

4. If there are more than one diagonal emanate from vertex- i , ($i \neq 1, 3$), first consider the diagonal that is closest to $(1, i)$ or $(3, i)$, If it is closer to $(1, i)$, then follow the rule that comes after $(1, i)$ (eq.(3.8)), else follow the rule that comes after $(3, i)$ (eq.(3.9)). Then the remaining correspondence can be determined by other rules.

To summarize, we first write down the propagator sequence according to Rule 1, then determine the corresponding differential operators according to other rules (among these, Rule 2 has the highest priority). Next, we provide some examples to help the readers understand better (we use blue arrows to represent the position of differential operators in the n -polygon and omit $[2, 2n], [1, 4]$).

Example 3.1. (4-point) In figure 3, for the scalar diagram $1/X_{1,5}$, we first write the propagator as $(1, 5)$, then according to (3.7), the corresponding differential operators is $[1, 6]$. For $1/X_{3,7}$, the propagator is $(3, 7)$ and the corresponding differential operator is $[3, 6]$, which are exactly eq.(3.3).

Example 3.2. (5-point) In figure 4, for the scalar diagram $1/X_{1,5}X_{5,9}$, we first write the propagator sequence as $(1, 5)(5, 9)$ (according to Rule 1, we require the sequence must be connected as closely as possible front and back), then according to (3.7) and (3.8), the corresponding differential operator is $[1, 6][5, 8]$.

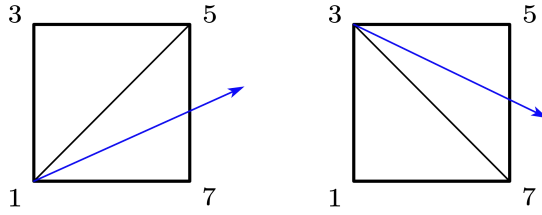


Figure 3: 4-point ϕ^3 diagrams and corresponding differential operators. The propagators are represented by black diagonals, while differential operators are indicated by blue arrows. For example, the operator $[1, 6]$ is depicted as an arrow starting from vertex-1 and pointing between vertices 5 and 7.

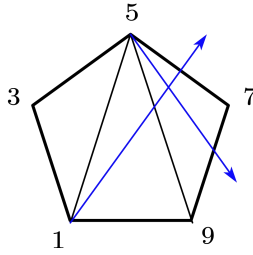


Figure 4: 5-point ϕ^3 diagram and corresponding differential operator.

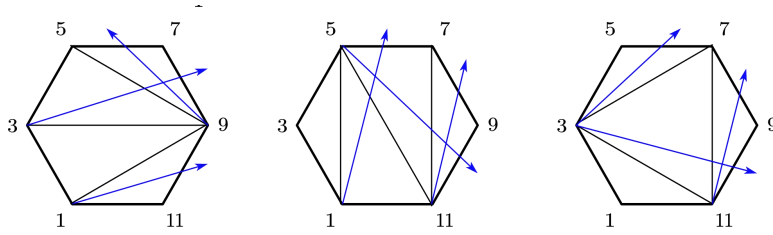


Figure 5: 6-point ϕ^3 diagrams and corresponding differential operators for ray-like, zigzag and cyclic triangulations.

Example 3.3. (6-point ray-like) In figure 5, for the scalar diagram $1/X_{1,9}X_{3,9}X_{5,9}$, we first write the propagator sequence as $(1, 9)(3, 9)(9, 5)$, then according to (3.7) and (3.9), the corresponding differential operator is $[1, 10][3, 8][9, 6]$.

Example 3.4. (6-point zigzag) In figure 5, for the scalar diagram $1/X_{1,5}X_{5,11}X_{7,11}$, we first write the propagator sequence as $(1, 5)(5, 11)(11, 7)$, then according to (3.7), (3.8) and (3.10), the corresponding differential operator is $[1, 6][5, 10][11, 8]$.

Example 3.5. (6-point cycle) In figure 5, for the scalar diagram $1/X_{3,7}X_{3,11}X_{7,11}$, according to Rule 1, the propagators now have a cycle structure $(3-7-11-3)$, since vertex-3 is in this cycle, so we should write the propagator sequence in a counterclockwise order: $(3, 11)(11, 7)(7, 3)$, then according to (3.7) and (3.9), the corresponding differential operator is $[3, 10][11, 8][6, 3]$.

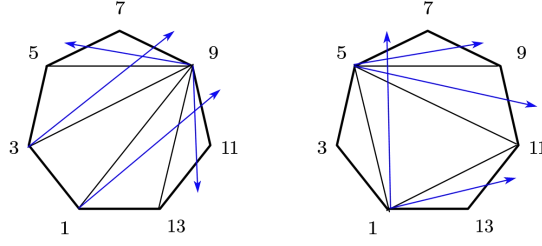


Figure 6: 7-point ϕ^3 diagrams and corresponding differential operators for ray-like and cyclic triangulations.

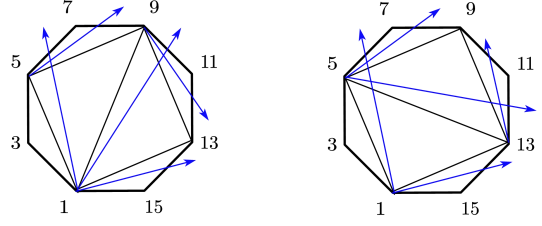


Figure 7: 8-point ϕ^3 diagrams and corresponding differential operators.

Example 3.6. (7-point ray-like) In figure 6, for the scalar diagram $1/X_{1,9}X_{3,9}X_{5,9}X_{9,13}$, note that $(5, 9)$ is closest to $(3, 9)$ and $(9, 13)$ is closest to $(1, 9)$, so according to Rule 4 we first write the propagator sequence as $(1, 9)(9, 13)(3, 9)(9, 5)$, then according to (3.7), (3.8) and (3.9), the corresponding differential operator is $[1, 10][9, 12][3, 8][9, 6]$.

Example 3.7. (7-point cycle) In figure 6, for the scalar diagram $1/X_{1,5}X_{1,11}X_{5,9}X_{5,11}$, according to Rule 1, the propagators now have a cycle structure $(1-5-11-1)$, since vertex-1 is in this cycle, so we should write the cycle in a clockwise order: $(1, 5)(5, 9)(5, 11)(11, 1)$, then according to (3.7), (3.8) and (3.10), the corresponding differential operator is $[1, 6][5, 8][5, 10][12, 1]$.

Example 3.8. (8-point cycle) In figure 7, for the scalar diagram $1/X_{1,5}X_{1,9}X_{1,13}X_{5,9}X_{9,13}$, according to Rule 1, the propagators now have two cycles $(1-5-9-1)$ and $(1-9-13-1)$, since vertex-1 is in this cycle, so we should write the cycles in a clockwise order: $(1, 5)(5, 9)(1, 9)(9, 13)(13, 1)$, then according to (3.7) and (3.8), the corresponding differential operator is $[1, 6][5, 8][1, 10][9, 12][14, 1]$. And for the scalar diagram $1/X_{1,5}X_{5,13}X_{1,13}X_{5,9}X_{9,13}$, according to Rule 1, the propagators now seem to have two cycles $(1-5-13-1)$ and $(5-9-13-5)$, but note that the second cycle does not contain vertex-1 or 3, so actually there is only one cycle. Since vertex-1 is in this cycle, so we should write the cycle in a clockwise order: $(1, 5)(5, 9)(5, 13)(13, 9)(13, 1)$, then according to (3.7), (3.8) and (3.10), the corresponding differential operator is $[1, 6][5, 8][5, 12][13, 10][14, 1]$.

Let us summarize the evident pattern for certain special topologies at general n .

Example 3.9. (n -point ray-like originating at vertices 1 and 3) For the scalar diagram

$$\frac{1}{X_{1,5}X_{1,7}X_{1,9} \cdots X_{1,2n-3}}, \quad (3.11)$$

the propagator sequence is $(1, 5)(1, 7)(1, 9) \cdots (1, 2n - 3)$ and the corresponding differential operator is given by $[1, 6][1, 8][1, 10] \cdots [1, 2n - 2]$.

Analogously, for the scalar diagram

$$\frac{1}{X_{3,7}X_{3,9}X_{3,11} \cdots X_{3,2n-1}}, \quad (3.12)$$

the propagator sequence is $(3, 7)(3, 9)(3, 11) \cdots (3, 2n - 1)$ and the corresponding differential operator is $[3, 6][3, 8][3, 10] \cdots [3, 2n - 2]$.

We will give a thorough proof of these two special cases in the next subsection.

Example 3.10. (n -point ray-like originating at vertices 5 and $2n - 1$) For the scalar diagram

$$\frac{1}{X_{5,1}X_{5,9}X_{5,11} \cdots X_{5,2n-1}}, \quad (3.13)$$

the propagator sequence is $(1, 5)(5, 2n - 1)(5, 2n - 3) \cdots (5, 9)$ and the corresponding differential operator is $[1, 6][5, 2n - 2][5, 2n - 4] \cdots [5, 8]$.

For the scalar diagram

$$\frac{1}{X_{2n-1,3}X_{2n-1,5}X_{2n-1,7} \cdots X_{2n-1,2n-5}}, \quad (3.14)$$

the propagator sequence is $(3, 2n - 1)(2n - 1, 5)(2n - 1, 7) \cdots (2n - 1, 2n - 5)$ and the corresponding differential operator is $[3, 2n - 2][2n - 1, 6][2n - 1, 8] \cdots [2n - 1, 2n - 4]$.

Example 3.11. (n -point ray-like originating at vertices 7 and $2n - 3$) For the scalar diagram

$$\frac{1}{X_{7,1}X_{7,3}X_{7,11} \cdots X_{7,2n-1}}, \quad (3.15)$$

the propagator sequence is $(3, 7)(1, 7)(7, 2n - 1)(7, 2n - 3) \cdots (7, 11)$ and the corresponding differential operator is $[3, 6][1, 8][7, 2n - 2][7, 2n - 4] \cdots [7, 10]$.

For the scalar diagram

$$\frac{1}{X_{2n-3,1}X_{2n-3,3}X_{2n-3,5} \cdots X_{2n-3,2n-7}}, \quad (3.16)$$

the propagator sequence is $(1, 2n - 3)(3, 2n - 3)(2n - 3, 5) \cdots (2n - 3, 2n - 7)$ and the corresponding differential operator is $[1, 2n - 2][3, 2n - 4][2n - 3, 6] \cdots [2n - 3, 2n - 6]$.

Example 3.12. (n -point ray-like) For the scalar diagram ($i \neq 1, 3, 5, 7, 2n - 3, 2n - 1$)

$$\frac{1}{X_{i,1}X_{i,3}X_{i,5} \cdots X_{i,i-4}X_{i,i+4} \cdots X_{i,2n-1}}, \quad (3.17)$$

according to Rule 4, we should write the propagator that is closest to $(1, i)$ or $(3, i)$, so the propagator sequence is $(1, i)(i, 2n - 1)(i, 2n - 3) \cdots (i, i + 4)(3, i)(i, 5)(i, 7) \cdots (i, i - 4)$ and the corresponding differential operator is $[1, i + 1][i, 2n - 2][i, 2n - 4] \cdots [i, i + 3][3, i - 1][i, 6][i, 8] \cdots [i, i - 3]$.

Example 3.13. (n -point zigzag starting from vertex-1) For the scalar diagram

$$\frac{1}{X_{1,5}X_{5,2n-1}X_{2n-1,7}X_{7,2n-3}\cdots}, \quad (3.18)$$

the propagator sequence is $(1, 5)(5, 2n - 1)(2n - 1, 7)(7, 2n - 3)\cdots$ and the corresponding differential operator is $[1, 6][5, 2n - 2][2n - 1, 8][7, 2n - 4]\cdots$.

For the scalar diagram

$$\frac{1}{X_{1,2n-3}X_{2n-3,3}X_{3,2n-5}X_{2n-5,5}X_{5,2n-7}\cdots}, \quad (3.19)$$

the propagator sequence is $(1, 2n - 3)(3, 2n - 3)(3, 2n - 5)(2n - 5, 5)(5, 2n - 7)\cdots$ and the corresponding differential operator is $[1, 2n - 2][3, 2n - 4][3, 2n - 6][2n - 5, 6][5, 2n - 8]\cdots$.

Example 3.14. (n -point one-flip from ray-like) For the scalar diagram

$$\frac{1}{X_{1,5}X_{1,7}X_{1,9}\cdots X_{2n-7,2n-3}X_{1,2n-3}}, \quad (3.20)$$

it is easy to see that in this case we just flip the $(1, 2n - 5)$ in the 1-ray-like to $(2n - 7, 2n - 3)$. Now the propagator sequence is $(1, 5)(1, 7)(1, 9)\cdots(1, 2n - 7)(2n - 7, 2n - 3)(1, 2n - 3)$ (note that after flipping, there is a cycle which has vertex-1 so we should write this cycle in a clockwise order) and the corresponding differential operator is $[1, 6][1, 8][1, 10]\cdots[1, 2n - 6][2n - 7, 2n - 4][1, 2n - 2]$.

3.2 Proof of the rules by factorization

We have presented the rules for constructing operators that extract single cubic diagrams from YM amplitudes. We now provide a proof of these rules, focusing on certain special cases at general multiplicity. The proof is divided into two main steps, based on factorization. First, for a given diagram, we show that the differential operator acting on the corresponding $(n - 3)$ consecutive factorizations (residues) yields 1. Second, we demonstrate that the same differential operator vanishes when acting on other consecutive factorizations associated with different diagrams. Each step is established recursively.

Let us begin by proving the validity of the operator associated with the ray-like diagram in which all vertices are connected to vertex-1.

Step I. We aim to show:

$$\mathcal{D}_{(2,2n),(1,4),(1,6),\dots,(1,2n-2)} \text{Res}_{X_{1,5}=X_{1,7}=\dots=X_{1,2n-3}=0} \mathcal{A}_n^{\text{YM}} = 1. \quad (3.21)$$

To begin with, consider the case $n = 4$, for which we have:

$$\begin{aligned} & \mathcal{D}_{(2,8),(1,4),(1,6)} \text{Res}_{X_{1,5}=0} \mathcal{A}_4(1, 2, \dots, 8), \quad (3.22) \\ & = \mathcal{D}_{(2,8),(1,4),(1,6)} \sum_{j,J} (X_{j,J} - X_{1,j} - X_{5,J}) \frac{\partial}{\partial X_{x,j}} \mathcal{A}_L(1, 2, 3, 4, 5, x) \frac{\partial}{\partial X_{x',J}} \mathcal{A}_R(5, 6, 7, 8, 1, x'), \end{aligned}$$

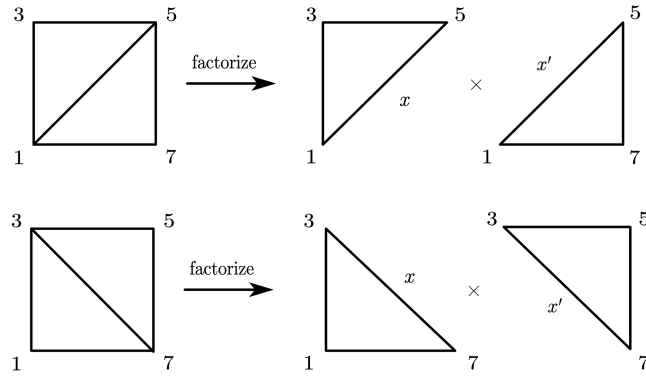


Figure 8: 4-point factorizations.

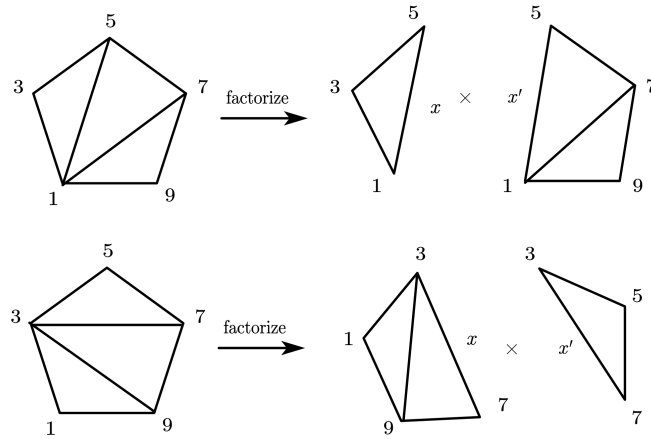


Figure 9: 5-point factorizations.

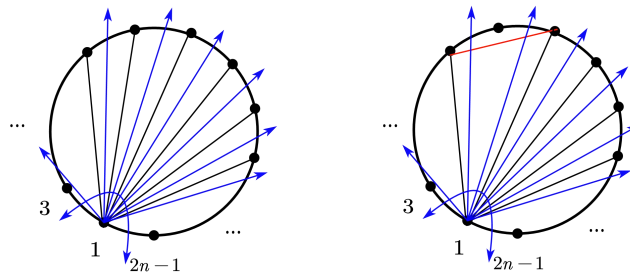


Figure 10: The number of vertex-1 ray-like intersections is $n - 3$ (left). In other cases, for example after one flip (denoted by the red line) from vertex-1 ray-like, the number of intersections is more than $n - 3$ (right).

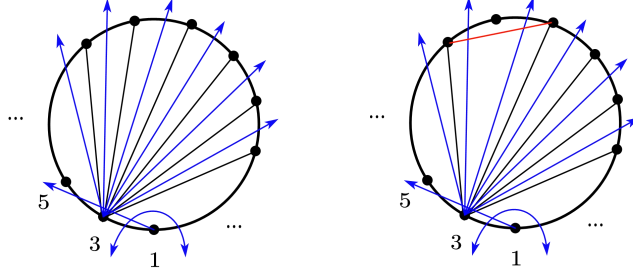


Figure 11: The number of vertex-3 ray-like intersections is $n - 3$ (left). In other cases, for example after one flip (denoted by the red line) from vertex-3 ray-like, the number of intersections is more than $n - 3$ (right).

where we have used (2.19), and the left and right 3-point subamplitudes are labeled by $(1, 2, 3, 4, 5, x)$ and $(5, 6, 7, 8, 1, x')$, respectively (figure 8). In this case, the derivative $\partial/\partial X_{2,8}$ must act on the prefactor, leading to:

$$\mathcal{D}_{(1,4),(1,6)} \frac{\partial}{\partial X_{x,2}} \mathcal{A}_L(1, 2, 3, 4, 5, x) \frac{\partial}{\partial X_{x',8}} \mathcal{A}_R(5, 6, 7, 8, 1, x') = 1. \quad (3.23)$$

In the final step, we have used the explicit expression (2.27) with the appropriate relabeling. Moving on to the case $n = 5$ (figure 9), we find:

$$\mathcal{D}_{(2,10),(1,4),(1,6),(1,8)} \sum_{j,J} (X_{j,J} - X_{1,j} - X_{5,J}) \frac{\partial}{\partial X_{x,j}} \mathcal{A}_L(1, 2, 3, 4, 5, x) \quad (3.24)$$

$$\times \text{Res}_{X_{1,7}=0} \frac{\partial}{\partial X_{x',J}} \mathcal{A}_R(5, 6, 7, 8, 9, 10, 1, x') \quad (3.25)$$

$$= \mathcal{D}_{(1,4),(1,6),(1,8)} \frac{\partial}{\partial X_{x,2}} \mathcal{A}_L(1, 2, 3, 4, 5, x) \times \text{Res}_{X_{1,7}=0} \frac{\partial}{\partial X_{x',10}} \mathcal{A}_R(5, 6, 7, 8, 9, 10, 1, x')$$

$$= \mathcal{D}_{(x',10),(1,6),(1,8)} \text{Res}_{X_{1,7}=0} \mathcal{A}(1, x', 5, 6, 7, 8, 9, 10) = 1.$$

In the second line, we have used the fact that $\partial/\partial X_{2,10}$ must act on the prefactor. In the final line, we have rewritten the result (after a cyclic relabeling of external legs) to match exactly with (3.22). This argument can be applied recursively to the general n -point case:

$$\begin{aligned} & \mathcal{D}_{(2,2n),(1,4),(1,6),\dots,(1,2n-2)} \text{Res}_{X_{1,5}=X_{1,7}=\dots=X_{1,2n-3}=0} \mathcal{A}_n^{\text{YM}}(1, 2, \dots, 2n) \quad (3.26) \\ &= \mathcal{D}_{(x',2n),(1,6),\dots,(1,2n-2)} \text{Res}_{X_{1,7}=X_{1,9}=\dots=X_{1,2n-3}=0} \mathcal{A}_{n-1}^{\text{YM}}(1, x', 5, 6, \dots, 2n) \\ &= \dots = 1. \end{aligned}$$

Step II. We now demonstrate:

$$\mathcal{D}_{(2,2n),(1,4),(1,6),\dots,(1,2n-2)} \text{Res}_{X_{i_1,j_1}=X_{i_2,j_2}=\dots=X_{i_{n-1},j_{n-1}}=0} \mathcal{A}_n^{\text{YM}} = 0, \quad (3.27)$$

for any sequence $(i_1, j_1)(i_2, j_2) \dots (i_{n-1}, j_{n-1}) \neq (1, 5)(1, 7) \dots (1, 2n - 3)$. In the previous

step, we saw that if a derivative involves a variable $X_{a,b}$ where a and b appear on opposite sides of a factorization channel, then that derivative must act on the prefactor in (2.19).

Now, suppose we draw the derivatives $[2, 2n], [1, 4], [1, 6], \dots, [1, 2n - 2]$ as blue lines, and the propagators $(i_1, j_1)(i_2, j_2) \dots (i_{n-1}, j_{n-1})$ as black lines. Then, for the derivative not to vanish, the number of intersections between blue and black lines must be at most $n - 3$. In figure 10, it is direct to find that there is only one such configuration with exactly $n - 3$ intersections, namely, when $(i_1, j_1)(i_2, j_2) \dots (i_{n-1}, j_{n-1}) = (1, 5)(1, 7) \dots (1, 2n - 3)$.

This completes the proof.

Following similar steps, we now prove the validity of the operator associated with the ray-like diagram in which all vertices are connected to vertex-3.

Step I. We aim to show:

$$\mathcal{D}_{(2,2n),(1,4),(3,6),(3,8),\dots,(3,2n-2)} \text{Res}_{X_{3,7}=X_{3,9}=\dots=X_{3,2n-1}=0} \mathcal{A}_n^{\text{YM}} = 1. \quad (3.28)$$

For the case $n = 4$, we have:

$$\begin{aligned} & \mathcal{D}_{(2,8),(1,4),(3,6)} \text{Res}_{X_{3,7}=0} \mathcal{A}_4(1, 2, \dots, 8), \quad (3.29) \\ = & \mathcal{D}_{(2,8),(1,4),(3,6)} \sum_{j,J} (X_{j,J} - X_{3,j} - X_{7,J}) \frac{\partial}{\partial X_{x,j}} \mathcal{A}_L(3, x, 7, 8, 1, 2) \frac{\partial}{\partial X_{x',J}} \mathcal{A}_R(3, 4, 5, 6, 7, x'), \end{aligned}$$

now the left and right 3-point subamplitudes are labeled by $(3, x, 7, 8, 1, 2)$ and $(3, 4, 5, 6, 7, x')$, respectively (figure 8). In this case, the derivative $\partial/\partial X_{1,4}$ must act on the prefactor, leading to:

$$\mathcal{D}_{(2,8),(3,6)} \frac{\partial}{\partial X_{x,1}} \mathcal{A}_L(3, x, 7, 8, 1, 2) \frac{\partial}{\partial X_{x',4}} \mathcal{A}_R(3, 4, 5, 6, 7, x') = 1. \quad (3.30)$$

In the final step, we have used the explicit expression (2.27) with the appropriate relabeling. For the case $n = 5$ (figure 9), we have:

$$\mathcal{D}_{(2,10),(1,4),(3,6),(3,8)} \sum_{j,J} (X_{j,J} - X_{3,j} - X_{7,J}) \frac{\partial}{\partial X_{x',j}} \mathcal{A}_R(3, 4, 5, 6, 7, x') \quad (3.31)$$

$$\times \text{Res}_{X_{3,9}=0} \frac{\partial}{\partial X_{x,J}} \mathcal{A}_L(3, x, 7, 8, 9, 10, 1, 2) \quad (3.32)$$

$$= \mathcal{D}_{(2,10),(3,6),(3,8)} \frac{\partial}{\partial X_{x',4}} \mathcal{A}_R(3, 4, 5, 6, 7, x') \times \text{Res}_{X_{3,9}=0} \frac{\partial}{\partial X_{x,1}} \mathcal{A}_L(3, x, 7, 8, 9, 10, 1, 2)$$

$$= \mathcal{D}_{(x,1),(2,10),(3,8)} \text{Res}_{X_{3,9}=0} \mathcal{A}(1, 2, 3, x, 7, 8, 9, 10) = 1.$$

In the second line, we have used the fact that $\partial/\partial X_{1,4}$ must act on the prefactor. In the final line, we have rewritten the result (after a cyclic relabeling of external legs) to match exactly with (3.29). This argument can be applied recursively to the general n -point case:

$$\begin{aligned} & \mathcal{D}_{(2,2n),(1,4),(3,6),(3,8),\dots,(3,2n-2)} \text{Res}_{X_{3,7}=X_{3,9}=\dots=X_{3,2n-1}=0} \mathcal{A}_n^{\text{YM}}(1, 2, \dots, 2n) \quad (3.33) \\ = & \mathcal{D}_{(x,1),(2,2n),(3,8),\dots,(3,2n-2)} \text{Res}_{X_{3,9}=X_{3,11}=\dots=X_{3,2n-1}=0} \mathcal{A}_{n-1}^{\text{YM}}(1, 2, 3, x, 7, 8, \dots, 2n) \\ = & \dots = 1. \end{aligned}$$

Step II. We now demonstrate:

$$\mathcal{D}_{(2,2n),(1,4),(3,6),(3,8)\dots,(3,2n-2)} \text{Res}_{X_{i_1,j_1}=X_{i_2,j_2}=\dots=X_{i_{n-1},j_{n-1}}=0} \mathcal{A}_n^{\text{YM}} = 0, \quad (3.34)$$

for any sequence $(i_1, j_1)(i_2, j_2) \dots (i_{n-1}, j_{n-1}) \neq (3, 7)(3, 9) \dots (3, 2n - 1)$. In figure 11, similar to the vertex-1 ray-like case, for the derivative not to vanish, the number of intersections between blue and black lines must be at most $n - 3$. It is direct to find that there is only one such configuration with exactly $n - 3$ intersections, namely, when $(i_1, j_1)(i_2, j_2) \dots (i_{n-1}, j_{n-1}) = (3, 7)(3, 9) \dots (3, 2n - 1)$.

This completes the proof.

4 Gluon Insertions and Minimal Basis

We have introduced a systematic method for extracting single-scalar cubic diagrams through differential operators. A natural question is whether there exist analogous operators that yield amplitudes containing gluons. In this section, we start by counting the number of independent “mixed amplitudes” generated by these operators. As we will see, planarity dictates that this number is given by \mathcal{C}_{r-2} , where r denotes the number of external scalar legs.

To be concrete, let us consider the number of linearly independent mixed amplitudes with chosen unordered gluons denoted by:

$$N_{n,r} = \dim \text{Span}\{\mathcal{A}_n^{\text{YM}+\phi^3}(\{\bar{\beta}\}|\beta)\}, \quad (4.1)$$

here $|\beta| = r$ denotes the number of scalars and $\{\bar{\beta}\}$ the complementary set of β , representing the gluons. Note that on the right hand side we have collected all possible permutations of β . It is clear that this number is independent of which particles are chosen as scalars, but only on their total number r ⁴. As we will see later, the number of gluons $n - r$, or equivalently the total number of particles n , is also irrelevant, *i.e.* we have $N_{n,r} = N_r$.

To illustrate, let us consider the case $n = 4$ with $r = 2, 3, 4$. Obviously, we have $N_{4,2} = N_{4,3} = 1$ due to the cyclic and reflection symmetries of the colored scalars. Furthermore, in the pure scalar case, *i.e.*, $r = 4$, the result is given by the number of 4-point ordered cubic diagrams: $N_{4,4} = 2$. In fact, at any given multiplicity we have $N_{n,2} = N_{n,3} = 1$ and $N_{n,n} = \mathcal{C}_{n-2}$.

The first nontrivial case appears at $n = 5$ with $r = 4$. Without loss of generality, we choose the scalars to be 1, 3, 4, 5, leaving 2 as the gluon. Taking into account the redundancies from cyclic and reflection symmetries, there are naively three equivalent orderings, namely

$$\{\mathcal{A}_5^{\text{YM}+\phi^3}(\{2\}|1, 3, 4, 5), \mathcal{A}_5^{\text{YM}+\phi^3}(\{2\}|1, 3, 5, 4), \mathcal{A}_5^{\text{YM}+\phi^3}(\{2\}|1, 4, 3, 5)\}. \quad (4.2)$$

⁴To provide simple examples, we only consider modding out the cyclic and reflection symmetries, the naive dimension is $\frac{(n-1)!}{2}$. One may further impose the Kleiss-Kuijff relation [16, 53] to fix two legs, reducing the naive dimension to $(n-2)!$. However, the actual number is much smaller than either of these.

Given the advantage of scaffolding variables, which provide a unique representation, we write

$$\mathcal{A}_5^{\text{YM}+\phi^3}(\{2\}|\beta) = n(\beta) \cdot \left\{ \frac{X_{4,9}}{X_{3,9}X_{5,9}}, \frac{X_{1,4}}{X_{1,5}X_{5,9}}, \frac{X_{4,7}}{X_{3,7}X_{3,9}}, \frac{X_{4,7}}{X_{1,7}X_{3,7}}, \frac{X_{1,4}}{X_{1,5}X_{1,7}}, \frac{1}{X_{5,9}}, \frac{1}{X_{3,9}}, \frac{1}{X_{1,7}} \right\},$$

where $n(\beta)$ is an 8-dimensional vector. Then we obtain the following matrix:

$$\begin{pmatrix} n(1, 3, 4, 5) \\ n(1, 3, 5, 4) \\ n(1, 4, 3, 5) \end{pmatrix} = \begin{pmatrix} -1 & -1 & -1 & -1 & -1 & 1 & 1 & 1 \\ 0 & 0 & 0 & 1 & 1 & 0 & 0 & -1 \\ 1 & 1 & 1 & 0 & 0 & -1 & -1 & 0 \end{pmatrix}, \quad (4.3)$$

where we have $n(1, 3, 4, 5) = -n(1, 3, 5, 4) - n(1, 4, 3, 5)$ and therefore the above matrix has rank 2. As a consequence, we find

$$N_{5,4} = 2. \quad (4.4)$$

Moving on to $n = 6$, there are two nontrivial cases with $r = 4$ and $r = 5$, respectively. For $r = 4$, one can similarly verify that the corresponding 3×74 matrix has rank 2. For $r = 5$, as shown in Appendix A.1, the 12×23 matrix has rank 5, and thus

$$N_{6,5} = \mathcal{C}_3 = 5. \quad (4.5)$$

So far we have experimentally found

$$N_r \equiv N_{n,r} = \mathcal{C}_{r-2}. \quad (4.6)$$

This is perhaps not surprising. Let us consider one step away from the pure scalar case, *i.e.*, with a single gluon insertion. For $n = 5$ with scalar 1, 3, 4, 5, there are two possible scalar skeletons (s and t channels), and the amplitude is obtained by inserting one gluon into these skeletons in all possible ways that preserve the overall ordering. That said, there exists a natural basis for such amplitudes:

$$\begin{aligned} \mathbf{A}_5^{\text{YM}+\phi^3}(\{2\}|1345) &= \mathcal{A}_5^{\text{YM}+\phi^3}(\{2\}|1, 3, 5, 4), \\ \mathbf{A}_5^{\text{YM}+\phi^3}(\{2\}|1[34]5) &= -\mathcal{A}_5^{\text{YM}+\phi^3}(\{2\}|1, 4, 3, 5), \end{aligned} \quad (4.7)$$

Here, $\mathbf{A}_5^{\text{YM}+\phi^3}(\{2\}|1345)$ and $\mathbf{A}_5^{\text{YM}+\phi^3}(\{2\}|1[34]5)$ denote the five-point mixed amplitudes with gluon 2 inserted into the scalar skeletons shown on the left and right of Figure 12, respectively. We use 1345 to label the diagram with no subtree on the line $(1, n)$, and 1[34]5 to label the diagram containing the subtree [34] on the same line. Such subtree structures correspond one-to-one with commutators. For later convenience, we also represent these amplitudes using a triangulated 5-gon. In this diagram, the edge (35) is marked with a purple double line to denote the gluon, while the black diagonal (15) separates the region into to an effective pure scalar subdiagram (1579). Furthermore, the red diagonals (17) and (59) are used to indicate the s - and t -channels, respectively ⁵.

⁵The red and black diagonals **do not** correspond to the final propagators after the gluon insertion.

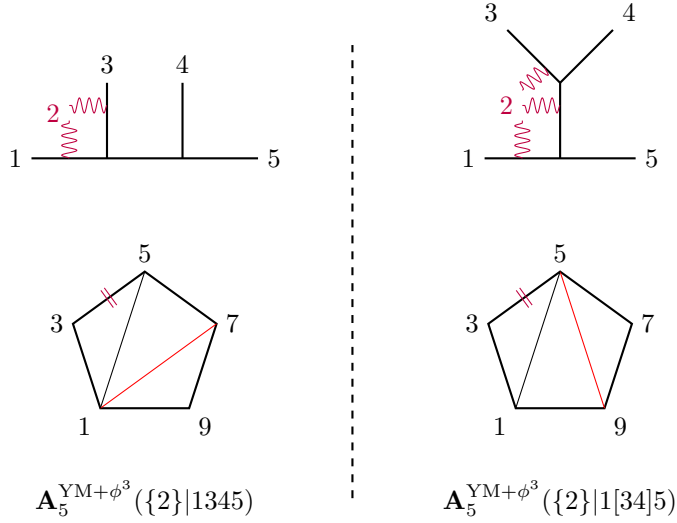


Figure 12: Single-gluon insertion at 5-point level, in which insertion in s and t -channels gives two independent amplitudes. In the pentagon, the red curves denote the propagators inherited from the 4-point skeleton diagrams, while the black ones separate out an effective scalar, yielding an equivalent lower-point pure scalar problem.

Similarly, the linear space for $n = 6$ with scalar 1, 2, 3, 4, 6 is spanned by (see Figure 13):

$$\begin{aligned} & \mathbf{A}_6^{\text{YM}+\phi^3}(\{5\}|12346), \mathbf{A}_6^{\text{YM}+\phi^3}(\{5\}|1[[23]4]6), \mathbf{A}_6^{\text{YM}+\phi^3}(\{5\}|1[2[34]]6), \\ & \mathbf{A}_6^{\text{YM}+\phi^3}(\{5\}|1[23]46), \mathbf{A}_6^{\text{YM}+\phi^3}(\{5\}|12[34]6) \end{aligned} \quad (4.8)$$

The above procedure strongly suggests that $N_{n,r}$ depends only on the number of scalars, as it effectively treats all possible gluon insertions into a given scalar skeleton as a single collective object. For example, as shown in Figure 14, for $n = 6$ with two gluons labeled by 2 and 4, the basis is given by:

$$\mathbf{A}_6^{\text{YM}+\phi^3}(\{2, 4\}|1356), \mathbf{A}_6^{\text{YM}+\phi^3}(\{2, 4\}|1[35]6). \quad (4.9)$$

We also provide a proof of the statement (4.6), which can be summarized as follows. Given the pure scalar case, where $N_{n,n} = \mathcal{C}_{n-2}$ is trivial, we consider the insertion of a single gluon into the mixed amplitudes. We then show that the dimension of the basis for such amplitudes remains the same as that of the amplitudes prior to the gluon insertion, by proving that their all-order soft limits are uniquely determined by the pre-insertion amplitudes. This constitutes a generalized uniqueness of the mixed amplitudes, analogous to the uniqueness of pure YM amplitudes [54].

To conclude this section, we remark that it is natural to choose the mixed amplitudes with gluons inserted into a single scalar skeleton as the basis for the corresponding linear space. As we will see later, in certain cases these amplitudes admit a straightforward generalization, represented by a single multi-derivative operator acting on the YM amplitudes,

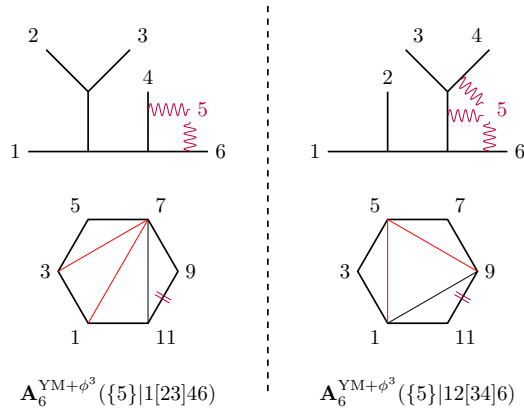
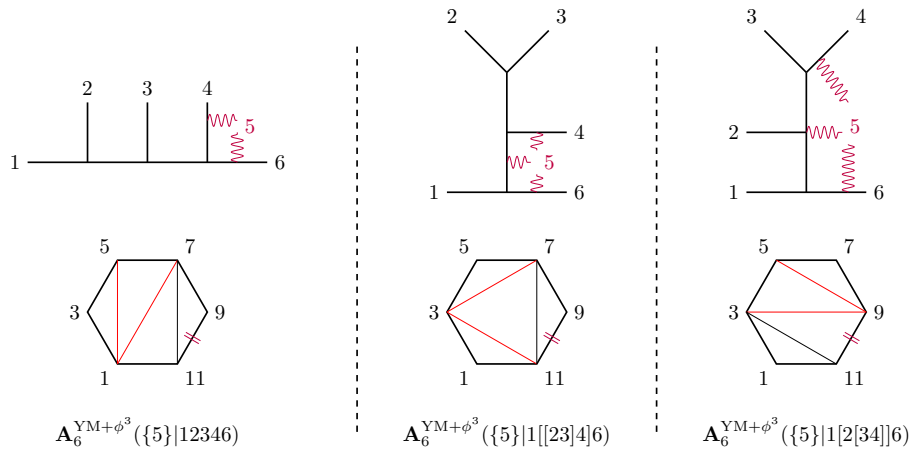


Figure 13: Single-gluon insertion for $n = 6$, with scalars being 1,2,3,4,6 and gluon being 5.

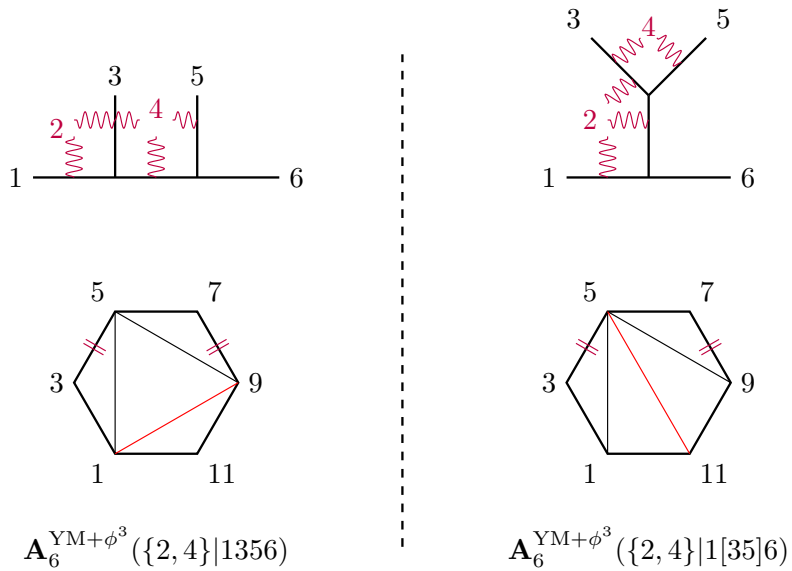


Figure 14: Double-gluon insertion at 6-point level, with inserted gluons being $\{2, 4\}$.

analogous to the pure scalar case. Moreover, this basis naturally spans a planar expansion of the original Yang-Mills amplitudes.

5 Gluon Insertions from Derivative

We have seen that the number of linearly independent building blocks for gluon and ϕ^3 scalar mixed amplitudes with r ($r \geq 2$) scalars is given by the Catalan number \mathcal{C}_{r-2} , which notably does not depend on the number of gluons. The linear space of mixed amplitudes with given gluons and scalars in different ordering is therefore spanned by the amplitudes of gluons inserted into single scalar diagram. This naturally leads to the question: can these amplitudes be obtained from pure Yang-Mills amplitudes by acting with suitable differential operators?

A naive approach would be to apply the chain rule to transform the operators in (2.39). However, this clearly results in linear combinations of multi-derivatives. It is therefore more desirable to study the behavior of single-term multi-derivatives, as they not only establish a direct connection between the pure gluon and mixed amplitudes, but also provide clearer structural control over the pure Yang-Mills amplitudes themselves. In this section, we present a simple answer: by following exactly the same rules as before (but with even fewer derivatives), one can obtain mixed amplitudes with gluons inserted into the scalar skeleton in infinitely many cases, while other types fail due to the violation of gauge invariance.

Starting with the pure YM amplitudes, it is clear that one needs to avoid derivatives involving $X_{2a,b}$ in order to preserve gluon a . In fact, the rule can be summarized as:

Given gluons labeled by a_1, a_2, \dots, a_s , the derivatives that extracted corresponding mixed amplitudes are determined by the rules introduced in Section 3, applied to the subpolygon obtained by deleting vertices $2a_1 - 1, 2a_1, 2a_2 - 1, 2a_2, \dots, 2a_s - 1, 2a_s$ from the original configuration.

The single scalar diagram we choose to obtain the operators in this smaller problem is precisely the skeleton into which we insert the gluons. Importantly, as we will explain later, preserving gauge invariance sometimes requires a **cyclic rotation** of the operators. Note that since there are exactly \mathcal{C}_{r-2} such diagrams (derivatives) on the subpolygon, this gives the number of independent basis elements! Let $\mathbf{A}_n^{\text{YM}+\phi^3}(\{a_1, \dots, a_s\}|g)$ denote the n -point mixed amplitude with gluons a_1, \dots, a_s inserted into the scalar diagram g , where the 2-scalar cases are denoted by $\mathbf{A}_n^{\text{YM}+\phi^3}(\{2, 3, \dots, n-1\}|1n)$ ⁶. We now provide examples to better illustrate this construction. For $n = 4$, aside from the pure gluon and pure scalar cases, we have the mixed cases with $r = 2$ and $r = 3$. For the former, the amplitude with particles 1 and 4 being scalars is given by $\mathbf{A}_4^{\text{YM}+\phi^3}(\{2, 3\}|14) = \mathcal{D}_{(2,8)}\mathcal{A}_4^{\text{YM}}$. For the latter, if particle 2 is a gluon, we consider an effective 3-point problem labeled by vertices 1, 2, 5, 6, 7, 8 See figure 15, and thus

$$\mathbf{A}_4^{\text{YM}+\phi^3}(\{2\}|134) = \mathcal{D}_{(2,8)(1,6)}\mathcal{A}_4^{\text{YM}}, \quad (5.1)$$

⁶For our purposes, when considering scalar amplitudes, we fix legs 1 and n to be scalars.

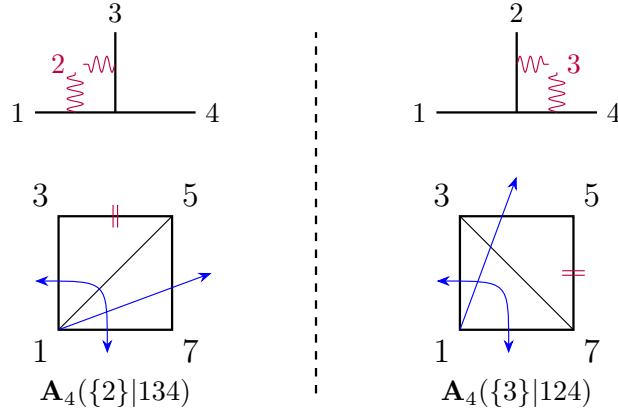


Figure 15: 4-point gluon insertions shown on Feynman diagrams and their dual polygons. The blue-arrowed curves denote the corresponding derivatives acting on $\mathcal{A}_4^{\text{YM}}$.

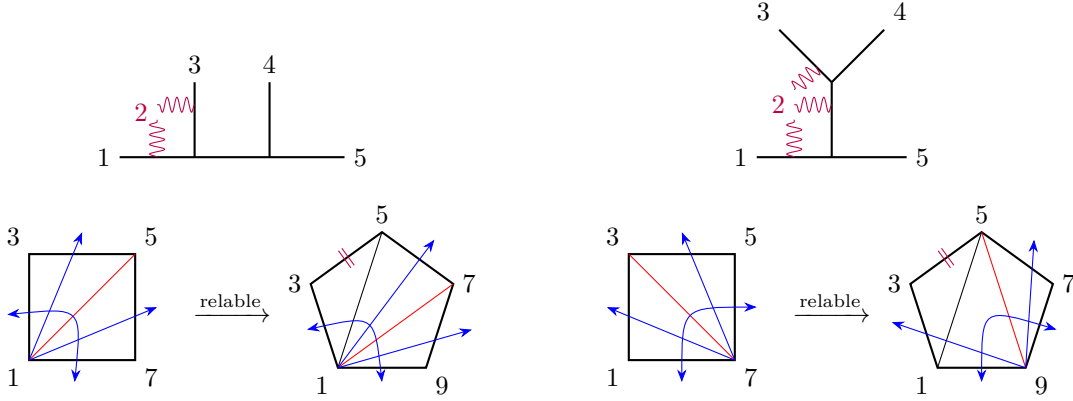


Figure 16: A 5-point mixed amplitude regarding “2” as the inserted gluon. The graphs on the left and right are taken from the contributions of 4-point s - and t -channels respectively.

and similarly

$$\mathbf{A}_4^{\text{YM}+\phi^3}(\{3\}|124) = \mathcal{D}_{(2,8)(1,4)}\mathcal{A}_4^{\text{YM}}. \quad (5.2)$$

It is clear that for general multiplicity with $r = 2, 3$ we have:

$$\mathbf{A}_n^{\text{YM}+\phi^3}(\{2, 3, \dots, n-1\}|1n) = \mathcal{D}_{(2,2n)}\mathcal{A}_n^{\text{YM}}, \quad (5.3)$$

and

$$\mathbf{A}_n^{\text{YM}+\phi^3}(\{2, 3, \dots, i-1, i+1, \dots, n-1\}|in) = \mathcal{D}_{(2,2n)(1,2i)}\mathcal{A}_n^{\text{YM}}. \quad (5.4)$$

Starting from 5-point, we encounter more nontrivial cases with $r = 4$. For instance, taking particle 2 to be the gluon, the effective scalar problem is labeled by $1, 2, 5, \dots, 10$. See figure 16. In this case, there are two contributing cubic diagrams, and the amplitudes are given by:

$$\mathbf{A}_5^{\text{YM}+\phi^3}(\{2\}|1345) = \mathcal{D}_{(2,10)(1,6)(1,8)}\mathcal{A}_5^{\text{YM}}, \quad (5.5)$$

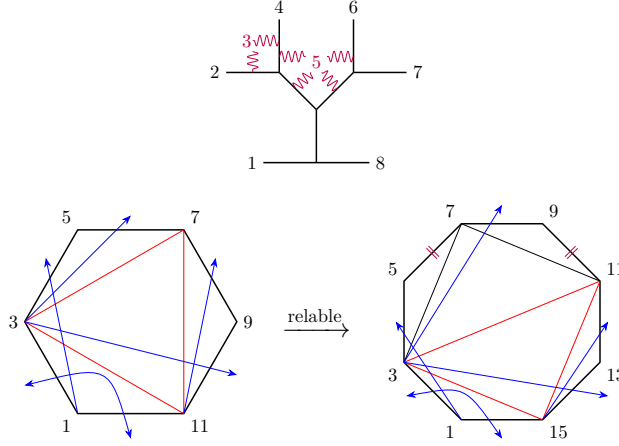


Figure 17: An 8-point example with gluons $\{3, 5\}$ inserted into a 6-point scalar graph.

where the operator $\mathcal{D}_{(2,10)(1,6)(1,8)}$ is a relabeling of $\mathcal{D}_{(2,8)(1,4)(1,6)}$. For diagram with propagator $1/X_{5,9}$ naively one expects the derivative to be $\mathcal{D}_{(2,10)(1,6)(5,8)}$ as the relabeling of $\mathcal{D}_{(2,8)(1,4)(3,6)}$. However, as we will explain shortly, we need to take its cyclic rotation and write:

$$\mathbf{A}_5^{\text{YM}+\phi^3}(\{2\}|1[34]5) = \mathcal{D}_{(8,10)(2,9)(6,9)}\mathcal{A}_5^{\text{YM}}. \quad (5.6)$$

Let us conclude by considering an 8-point example with 2 gluons and 6 scalars:

$$\mathbf{A}_8^{\text{YM}+\phi^3}(\{3, 5\}|1[24][67]8) = \mathcal{D}_{(2,16)(1,4)(3,14)(15,12)(8,3)}\mathcal{A}_8^{\text{YM}}. \quad (5.7)$$

where the operator above is obtained by relabeling of $\mathcal{D}_{(2,12)(1,4)(3,10)(11,8)(6,3)}$ from $1, 2, \dots, 12$ to $1, 2, 3, 4, 7, 8, 11, 12, \dots, 15, 16$. See figure 17. Next we provide strong consistency check by proving certain operators obtained this way in general multiplicity is gauge invariant (and multi-linear) in remaining gluons. For simplicity we define:

$$\mathcal{W}_{2i} \equiv \sum_{j \neq i-1, i, i+1} (X_{2i,j} - X_{2i-1,j})\mathcal{D}_{(2i,j)}, \quad (5.8)$$

and

$$\tilde{\mathcal{W}}_{2i} \equiv \sum_{j \neq i-1, i, i+1} (X_{2i,j} - X_{2i+1,j})\mathcal{D}_{(2i,j)}. \quad (5.9)$$

Thus the gauge invariance and multi-linearity conditions (2.16) and (2.17) read ⁷:

$$\mathcal{W}_{2i}\mathcal{A}_n^{\text{YM}} = \tilde{\mathcal{W}}_{2i}\mathcal{A}_n^{\text{YM}} = \mathcal{A}_n^{\text{YM}}. \quad (5.10)$$

Given an operator \mathcal{D}_ρ that does **not** involve the even labels $2i_1, 2i_2, \dots, 2i_s$, it preserves gauge invariance if:

$$\mathcal{W}_{2i}\mathcal{D}_\rho\mathcal{A}_n^{\text{YM}} - \mathcal{D}_\rho\mathcal{A}_n^{\text{YM}} = 0, \quad (5.11)$$

⁷In the following we simply refer to gauge invariance and multi-linearity as gauge invariance.

and

$$\tilde{\mathcal{W}}_{2i} \mathcal{D}_\rho \mathcal{A}_n^{\text{YM}} - \mathcal{D}_\rho \mathcal{A}_n^{\text{YM}} = 0, \quad (5.12)$$

for $i = i_1, i_2, \dots, i_s$. Using (5.10) the above conditions are equivalent to requiring the following commutators vanish:

$$[\mathcal{W}_{2i}, \mathcal{D}_\rho] = [\tilde{\mathcal{W}}_{2i}, \mathcal{D}_\rho] = 0. \quad (5.13)$$

It is easy to verify that for $\rho = (2a, 2b)$, equation (5.13) holds for any $i \neq a, b$. Naturally, no operator can extract an object that is gauge invariant at $(n - 1)$ points. Now consider $\rho = (2a, 2b - 1)$ and choose $i = b$, the commutator yields:

$$\begin{aligned} [\mathcal{W}_{2b}, \mathcal{D}_{(2a, 2b-1)}] &= (X_{2a, 2b} - X_{2a, 2b-1}) \mathcal{D}_{(2a, 2b)} \mathcal{D}_{(2a, 2b-1)} - \mathcal{D}_{(2a, 2b)} (X_{2a, 2b} - X_{2a, 2b-1}) \mathcal{D}_{(2a, 2b-1)} \\ &= -\mathcal{D}_{(2a, 2b-1)}. \end{aligned} \quad (5.14)$$

In the first line, we have used the fact that only the term with $j = 2a$ survives in the summation within \mathcal{W}_{2b} . And in the second line, we have used the linearity in the even label $2a$, as given in equation (3.1). In fact, it is straightforward to find:

$$[\mathcal{W}_{2i}, \mathcal{D}_{(2a, 2b-1)}] = -\delta_{i, b} \mathcal{D}_{(2a, 2b-1)}, \quad (5.15)$$

$$[\tilde{\mathcal{W}}_{2i}, \mathcal{D}_{(2a, 2b+1)}] = -\delta_{i, b} \mathcal{D}_{(2a, 2b+1)}. \quad (5.16)$$

Therefore, for a derivative of the form $\mathcal{D}_{(2a, 2b-1)}$, which involves one even label $2a$ and one odd label $2b - 1$, the gauge invariance associated with particles b and $b - 1$ corresponding to even labels $2b$ and $2b - 2$ is broken. This can be compensated by introducing $\mathcal{D}_{(2b, 2b-2)}$ to effectively “remove” these gluons. This is precisely the mechanism used in constructing the 3-scalar amplitude with derivatives $\mathcal{D}_{(2, 2n), (1, 2a)}$, where 2 and $2n$ are adjacent to 1. And more generally, we have:

$$[\mathcal{W}_{2i}, \mathcal{D}_{(2a', 2b'), (2a_1, 2b_1-1), \dots, (2a_m, 2b_m-1)}] = [\tilde{\mathcal{W}}_{2i}, \mathcal{D}_{(2a', 2b'), (2a_1, 2b_1-1), \dots, (2a_m, 2b_m-1)}] = 0. \quad (5.17)$$

for all $i \neq a', b', a_1, a_2, \dots, a_m$ if

$$(2b_1 - 1) \pm 1, (2b_2 - 1) \pm 1, \dots, (2b_m - 1) \pm 1 \in \{2a', 2b', 2a_1, 2a_2, \dots, 2a_m\}. \quad (5.18)$$

In other words, every label adjacent to an odd index in the derivative must also appear as an even label within it.

Now, returning to the example (5.6) discussed earlier, we see that the derivative $\mathcal{D}_{(8, 10)(2, 9)(6, 9)}$ satisfies the condition, since the labels 8 and 10, which are adjacent to 9, appear in the derivative. In contrast, the expression before the cyclic rotation, namely $\mathcal{D}_{(2, 10)(1, 6)(5, 8)}$, does not satisfy the condition: here, the presence of odd labels 1 and 5 requires that their adjacent even labels 2, 10, 4, 6 all appear, however, label 4 is missing.

It is easy to verify that our construction works for all $r = 2, 3, \dots, n$ up to $n = 8$. However, the first counterexamples appear at $n = 9$. For instance, consider inserting

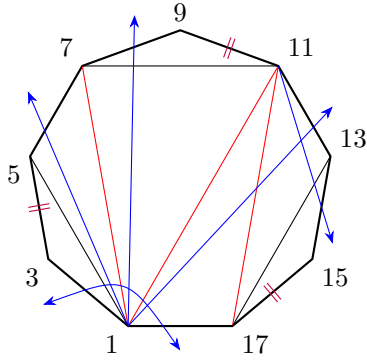


Figure 18: A 9-point mixed amplitude with gluons $\{2, 4, 6\}$ inserted into the scalar diagram 1235[78]9 along with its corresponding derivative fails to preserve the gauge invariance of gluon 6.

gluons 2, 5, 8 into the scalar diagram 134[67]9, as shown in Figure 18. The best one can do in this case is to construct the operator $\mathcal{D}_{(2,18)(1,6)(1,8)(1,12)(11,14)}$. However, gauge invariance for gluon 6 is broken due to the presence of the derivative $\partial/\partial X_{11,14}$. In fact, we have:

$$[\mathcal{W}_{2i}, \mathcal{D}_{(2,18)(1,6)(1,8)(1,12)(11,14)}] = -\mathcal{D}_{(2,18)(1,6)(1,8)(1,12)(12,14)}. \quad (5.19)$$

It would be interesting to study general operators, or combinations thereof, that preserve gauge invariance in this context; we leave this investigation for future work.

6 The Planar Universal Expansion

The lesson from the previous sections is that the optimal asymptotic behavior of the number of terms in an expansion for gluon amplitudes should not go beyond Catalan number. A natural application of this observation is to rewrite the universal expansion (2.40) in terms of the basis we have discussed:

$$\mathcal{A}_n^{\text{YM}} = \sum_{m, 1g_{\{\alpha\}}n} (-1)^m W(1g_{\{\alpha\}}n) \mathbf{A}_n^{\text{YM}+\phi^3}(\{\bar{\alpha}\}|1g_{\{\alpha\}}n), \quad (6.1)$$

where the sum runs over all unordered subsets α of $2, 3, \dots, n$ with $|\alpha| = m$. For each subset, we further sum over \mathcal{C}_m scalar cubic graphs $1g_{\{\alpha\}}n$, labeled by commutators that correspond to subtrees along the $(1, n)$ line. In this rewritten form, the original prefactor acquires precisely the same commutator structure (c.f. [55]) and the new prefactor is denoted by $W(1g_{\{\alpha\}}n)$. For example:

$$\begin{aligned} W(123456) &= \epsilon_1 \cdot f_2 \cdot f_3 \cdot f_4 \cdot f_5 \cdot \epsilon_6, & W(1[23]456) &= \epsilon_1 \cdot f_{[2 \cdot f_3]} \cdot f_4 \cdot f_5 \cdot \epsilon_6, \\ W(1[[23]4]56) &= \epsilon_1 \cdot f_{[[2 \cdot f_3] \cdot f_4]} \cdot f_5 \cdot \epsilon_6, & W(1[[23][45]]6) &= \epsilon_1 \cdot f_{[[2 \cdot f_3] \cdot f_{[4 \cdot f_5]]}] \cdot \epsilon_6. \end{aligned}$$

One can of course express the prefactor in terms of the scalar-scaffolded variables. Note that [56]:

$$f_i^{\mu\nu} = k_i^{[\mu} \epsilon_i^{\nu]} = -(p_{2i-1} + p_{2i})^{[\mu} p_{2i-1}^{\nu]} = p_{2i-1}^{[\mu} p_{2i}^{\nu]}, \quad (6.2)$$

where we have used the gauge choice $\lambda = 0$ in (2.6)⁸. We can then express the original prefactor as the following commutator:

$$\epsilon_1 \cdot f_{\alpha_1} \cdot f_{\alpha_2} \cdots f_{\alpha_m} \cdot \epsilon_n = s_{1,[2\alpha_1-1]s_{2\alpha_1+1],[2\alpha_2-1]s_{2\alpha_2],[2\alpha_3-1} \cdots s_{2\alpha_m}],2n-1}, \quad (6.3)$$

where $s_{i,j} = (p_i + p_j)^2 = 2p_i \cdot p_j$. We have omitted a factor of $(1/2)^{2m+1}$ as well as that could appear in the mixed amplitude, which can be absorbed into the definition of the coupling constant. The prefactor $W(1, g_\alpha, n)$ is then constructed as a nested commutator built upon this structure. Let us present the explicit expansion for $n = 4, 5$.

For $n = 4$, the original amplitudes are reorganized as:

$$\mathcal{A}_4^{\text{YM}+\phi^3}(\{2, 3\}|1, 4) = \mathbf{A}_4^{\text{YM}+\phi^3}(\{2, 3\}|14), \quad (6.4)$$

$$\mathcal{A}_4^{\text{YM}+\phi^3}(\{3\}|1, 2, 4) = \mathbf{A}_4^{\text{YM}+\phi^3}(\{3\}|124), \quad (6.5)$$

$$\mathcal{A}_4^{\text{YM}+\phi^3}(\{2\}|1, 3, 4) = \mathbf{A}_4^{\text{YM}+\phi^3}(\{2\}|134), \quad (6.6)$$

$$\mathcal{A}_4^{\text{YM}+\phi^3}(\emptyset|1, 2, 3, 4) = \mathbf{A}_4^{\text{YM}+\phi^3}(\emptyset|1234) + \mathbf{A}_4^{\text{YM}+\phi^3}(\emptyset|1[23]4), \quad (6.7)$$

$$\mathcal{A}_4^{\text{YM}+\phi^3}(\emptyset|1, 3, 2, 4) = -\mathbf{A}_4^{\text{YM}+\phi^3}(\emptyset|1[23]4). \quad (6.8)$$

Plugging the above results into (2.42) we find:

$$\begin{aligned} \mathcal{A}_4^{\text{YM}} &= W(14) \mathbf{A}_4^{\text{YM}+\phi^3}(\{2, 3\}|14) \\ &\quad - W(124) \mathbf{A}_4^{\text{YM}+\phi^3}(\{3\}|124) - W(134) \mathbf{A}_4^{\text{YM}+\phi^3}(\{2\}|134) \\ &\quad + W(1234) \mathbf{A}_4^{\text{YM}+\phi^3}(\emptyset|1234) + W(1[23]4) \mathbf{A}_4^{\text{YM}+\phi^3}(\emptyset|1[23]4). \end{aligned} \quad (6.9)$$

Similarly, for $n = 5$ we have (see Appendix B for details):

$$\begin{aligned} \mathcal{A}_5^{\text{YM}} &= W(15) \mathbf{A}_5^{\text{YM}+\phi^3}(\{2, 3, 4\}|15) - W(125) \mathbf{A}_5^{\text{YM}+\phi^3}(\{3, 4\}|125) \\ &\quad - W(135) \mathbf{A}_5^{\text{YM}+\phi^3}(\{2, 4\}|135) - W(145) \mathbf{A}_5^{\text{YM}+\phi^3}(\{2, 3\}|145) \\ &\quad + W(1235) \mathbf{A}_5^{\text{YM}+\phi^3}(\{4\}|1235) + W(1[23]5) \mathbf{A}_5^{\text{YM}+\phi^3}(\{4\}|1[23]5) \\ &\quad + W(1245) \mathbf{A}_5^{\text{YM}+\phi^3}(\{3\}|1245) + W(1[24]5) \mathbf{A}_5^{\text{YM}+\phi^3}(\{3\}|1[24]5) \\ &\quad + W(1345) \mathbf{A}_5^{\text{YM}+\phi^3}(\{2\}|1345) + W(1[34]5) \mathbf{A}_5^{\text{YM}+\phi^3}(\{2\}|1[34]5) \\ &\quad - W(12345) \mathbf{A}_5^{\text{YM}+\phi^3}(\emptyset|12345) - W(1[[23]4]5) \mathbf{A}_5^{\text{YM}+\phi^3}(\emptyset|1[[23]4]5) \\ &\quad - W(12[34]5) \mathbf{A}_5^{\text{YM}+\phi^3}(\emptyset|12[34]5) - W(1[23]45) \mathbf{A}_5^{\text{YM}+\phi^3}(\emptyset|1[23]45) \\ &\quad - W(1[2[34]]5) \mathbf{A}_5^{\text{YM}+\phi^3}(\emptyset|1[2[34]]5). \end{aligned} \quad (6.10)$$

⁸In our convention, we take $\epsilon_i = -p_{2i-1}$, whereas Ref. [56] adopts $\epsilon_i = p_{2i-1}$.

Note that the number of terms in this planar universal expansion is given by:

$$\sum_{m=0}^{n-2} \mathcal{C}_m \binom{n-2}{m}, \quad (6.11)$$

which takes the values 2, 5, 15, 51, 188, 731 for $n = 3, 4, 5, 6, 7, 8$, and asymptotically grows as $5^{n+1/2}/(8\sqrt{\pi} n^{3/2})$ for large n (see (OEIS A007317)).

It would be interesting to further investigate the expansion of the mixed amplitudes within the planar universal expansion. If one follows the reference ordering dependent approach of [7, 9], the final result, of course, reproduces their expressions, yielding the (commutators of) BCJ numerators multiplied by pure scalar diagrams. However, we remark that our formulation involves fewer terms at each intermediate step. For example, for the $(n-2)$ -gluon amplitudes, one finds:

$$\begin{aligned} \mathcal{A}_n^{\text{YM}+\phi^3}(\{2, 3, \dots, n-1\}|1n) &= \mathbf{A}_n^{\text{YM}+\phi^3}(\{2, 3, \dots, n-1\}|1n) \\ &= \sum_{s, \beta} \tilde{W}(\beta; 2) \mathcal{A}_n^{\text{YM}+\phi^3}(\{\bar{\beta}\}|1\beta^{-1}2n), \end{aligned} \quad (6.12)$$

where further choose leg 2 to be special and sum over the ordered subsets β with $|\beta| = s$ and β^{-1} to be its reverse ordered set. The prefactor $\tilde{W}(\beta; 2)$ is defined by

$$\tilde{W}(\beta; 2) = \epsilon_2 \cdot f_{\beta_1} \cdot f_{\beta_2} \cdots f_{\beta_s} \cdot k_1, \quad (6.13)$$

or equivalently

$$\begin{aligned} \tilde{W}(\beta; 2) &= s_{1, [2\beta_1-1] s_{2\beta_1+1}, [2\beta_2-1] s_{2\beta_2}, [2\beta_3-1] \cdots s_{2\beta_s}, 3} \\ &\quad + s_{2, [2\beta_1-1] s_{2\beta_1+1}, [2\beta_2-1] s_{2\beta_2}, [2\beta_3-1] \cdots s_{2\beta_s}, 3} \end{aligned} \quad (6.14)$$

in the scalar scaffolded kinematics. Rewriting the above expression in our basis gives:

$$\mathbf{A}_n^{\text{YM}+\phi^3}(\{2, 3, \dots, n-1\}|1n) = \sum_{s, 1g_{(2\beta)}n} (-1)^s \tilde{W}(g_{(\beta)}; 2) \mathbf{A}_n^{\text{YM}+\phi^3}(\{\bar{\beta}\}|1g_{(2\beta)}n), \quad (6.15)$$

where $1g_{(2\beta)}n$ denotes the graphs corresponding to the full commutator that includes 2 and β , while $g_{(\beta)}$ in $g_{(\beta)}; 2$ represents the associated commutator without 2. For instance, the 5-point 3 gluons amplitude is given by:

$$\begin{aligned} \mathbf{A}_n^{\text{YM}+\phi^3}(\{2, 3, 4\}|15) &= \tilde{W}(\emptyset; 2) \mathbf{A}_n^{\text{YM}+\phi^3}(\{34\}|125) \\ &\quad - \tilde{W}(3; 2) \mathbf{A}_n^{\text{YM}+\phi^3}(\{4\}|1[23]5) - \tilde{W}(4; 2) \mathbf{A}_n^{\text{YM}+\phi^3}(\{3\}|1[24]5) \\ &\quad + \tilde{W}(34; 2) \mathbf{A}_n^{\text{YM}+\phi^3}(\emptyset|1[[23]4]5) + \tilde{W}([34]; 2) \mathbf{A}_n^{\text{YM}+\phi^3}(\emptyset|1[2[34]5]). \end{aligned} \quad (6.16)$$

We expect to develop a different approach that eliminates reference-ordering dependence while manifestly preserving the planar structure for both pure YM and mixed amplitudes. We leave this for future work.

7 Conclusions and Outlook

In this work, we have revisited and explored some structural aspects of Yang-Mills amplitudes written in scaffolding variables. By analyzing their factorizations, we developed a systematic prescription for constructing differential operators that map the gluon amplitudes into single cubic scalar diagrams. We also considered a naive generalization of this construction to obtain the mixed amplitudes of gluons and scalars, which succeeds/fails in infinite cases of given types. We showed that the mixed amplitude with r scalars and any number of gluons admits a natural basis consisting of \mathcal{C}_{r-2} elements. We then applied this result to construct a planar version of the universal expansion, in which each term consists of a gauge-invariant prefactor expressed as a nested commutator, accompanied by the mixed amplitudes defined in our basis.

There remains several directions for future investigation. First, it would be interesting to further study the structure of the differential operators that preserve gauge invariance in the scaffolding variables and present a complete set of differential operators that generate all mixed amplitudes in this planar basis. In addition, developing new approach that fully manifests the planar structure for mixed amplitudes would represent a natural next step toward a more universal understanding of YM amplitudes (see [57] for a recent paper on new recursion of scalar-scaffolded pure YM).

Moreover, our results hint at broader applicability beyond YM theory. Since all colored amplitudes, such as those in the Nonlinear Sigma Model, colored Yukawa theory [58], and even certain subsets of the mixed amplitudes involving gravitons, gluons, and scalars, exhibit similar structures [59], understanding whether the differential-operator methods developed here can be extended to these theories would shed light on the universality of the scaffolded approach.

Finally, it would be very interesting to extend our analysis beyond tree level or into theories with richer matter content (c.f. [60–65] for recent works on one-loop field theory and string amplitudes). An immediate next step is to investigate whether an analogue of our planar expansion exists at one loop [62].

Acknowledgments

It is our pleasure to thank Song He for stimulating discussions, encouragement and collaborations on the early stage of this project. We also thank Qu Cao and Fan Zhu for discussions. The work of JD is supported by the DFG grant 508889767, Forschungsgruppe “Modern foundations of scattering amplitudes”.

A Details of Minimal Basis for Mixed Amplitudes

A.1 6-point 2-gluon examples

We provide an explicit example to demonstrate that $N_{6,5} = 5$. Without loss of generality, we choose the only gluon to be 5 and define:

$$\begin{aligned}
& \mathcal{A}_6^{\text{YM}+\phi^3}(\{5\}|\beta) \\
&= n(\beta) \cdot \left(\frac{X_{7,10}}{X_{3,11}X_{5,11}X_{7,11}}, \frac{X_{7,10}}{X_{1,5}X_{5,11}X_{7,11}}, \frac{X_{7,10}}{X_{3,7}X_{3,11}X_{7,11}}, \frac{X_{7,10}}{X_{1,7}X_{3,7}X_{7,11}}, \frac{X_{7,10}}{X_{1,5}X_{1,7}X_{7,11}}, \right. \\
& \quad \frac{X_{5,10}}{X_{3,11}X_{5,9}X_{5,11}}, \frac{X_{5,10}}{X_{1,5}X_{5,9}X_{5,11}}, \frac{X_{3,10}}{X_{3,9}X_{3,11}X_{5,9}}, \frac{X_{1,10}}{X_{1,9}X_{3,9}X_{5,9}}, \frac{X_{1,10}}{X_{1,5}X_{1,9}X_{5,9}}, \frac{X_{3,10}}{X_{3,7}X_{3,9}X_{3,11}}, \\
& \quad \frac{X_{1,10}}{X_{1,9}X_{3,7}X_{3,9}}, \frac{X_{1,10}}{X_{1,7}X_{1,9}X_{3,7}}, \frac{X_{1,10}}{X_{1,5}X_{1,7}X_{1,9}}, \frac{1}{X_{3,11}X_{5,11}}, \frac{1}{X_{1,5}X_{5,11}}, \frac{1}{X_{3,11}X_{5,9}}, \\
& \quad \left. \frac{1}{X_{3,9}X_{5,9}}, \frac{1}{X_{1,5}X_{5,9}}, \frac{1}{X_{3,7}X_{3,11}}, \frac{1}{X_{3,7}X_{3,9}}, \frac{1}{X_{1,7}X_{3,7}}, \frac{1}{X_{1,5}X_{1,7}} \right). \tag{A.1}
\end{aligned}$$

Note that in this case there are 12 cyclic and reflection inequivalent orderings, namely:

$$\begin{aligned}
& \{(1, 2, 3, 4, 6), (1, 2, 3, 6, 4), (1, 2, 4, 3, 6), (1, 2, 4, 6, 3), (1, 2, 6, 3, 4), (1, 2, 6, 4, 3), \\
& (1, 3, 2, 4, 6), (1, 3, 2, 6, 4), (1, 3, 4, 2, 6), (1, 3, 6, 2, 4), (1, 4, 2, 3, 6), (1, 4, 3, 2, 6)\}. \tag{A.2}
\end{aligned}$$

The corresponding 12×23 matrix is then given by:

$$\begin{pmatrix}
-1 & -1 & -1 & -1 & -1 & -1 & -1 & -1 & -1 & -1 & -1 & -1 & -1 & 1 & 1 & 1 & 1 & 1 & 1 & 1 & 1 & 1 \\
0 & 0 & 0 & 1 & 1 & 0 & 0 & 0 & 0 & 0 & 0 & 0 & 1 & 1 & 0 & 0 & 0 & 0 & 0 & 0 & -1 & -1 \\
1 & 1 & 0 & 0 & 0 & 1 & 1 & 1 & 1 & 1 & 0 & 0 & 0 & 0 & -1 & -1 & -1 & -1 & 0 & 0 & 0 & 0 \\
0 & 0 & 0 & 0 & 1 & 0 & 0 & 0 & 0 & 0 & 0 & 0 & 0 & 1 & 0 & 0 & 0 & 0 & 0 & 0 & 0 & -1 \\
0 & 1 & 0 & 0 & 0 & 0 & 1 & 0 & 0 & 1 & 0 & 0 & 0 & 0 & 0 & -1 & 0 & 0 & -1 & 0 & 0 & 0 \\
0 & -1 & 0 & 0 & -1 & 0 & -1 & 0 & 0 & -1 & 0 & 0 & 0 & -1 & 0 & 1 & 0 & 0 & 1 & 0 & 0 & 1 \\
0 & 0 & 1 & 1 & 0 & 0 & 0 & 0 & 0 & 0 & 1 & 1 & 1 & 0 & 0 & 0 & 0 & 0 & 0 & -1 & -1 & -1 \\
0 & 0 & 0 & -1 & 0 & 0 & 0 & 0 & 0 & 0 & 0 & 0 & -1 & 0 & 0 & 0 & 0 & 0 & 0 & 0 & 1 & 0 \\
1 & 0 & 0 & 0 & 0 & 1 & 0 & 1 & 1 & 0 & 0 & 0 & 0 & 0 & -1 & 0 & -1 & -1 & 0 & 0 & 0 & 0 \\
0 & 0 \\
0 & 0 & 1 & 0 & 0 & 0 & 0 & 0 & 0 & 0 & 1 & 1 & 0 & 0 & 0 & 0 & 0 & 0 & 0 & -1 & -1 & 0 \\
-1 & 0 & -1 & 0 & 0 & -1 & 0 & -1 & -1 & 0 & -1 & -1 & 0 & 0 & 1 & 0 & 1 & 1 & 0 & 1 & 1 & 0
\end{pmatrix}$$

and one can readily verify that this matrix has rank 5.

A.2 Proof

In this appendix, we prove the number of linearly independent mixed amplitudes with r scalars and $n - r$ gluons is \mathcal{C}_{r-2} . We start with an ansatz keeping identical propagators with

the mixed amplitudes (i.e. obeying locality), denoted as

$$M_n(p^l) = \sum_g \frac{\mathcal{M}_g(p^l)}{\prod_i P_{g,i}}, \quad (\text{A.3})$$

in which the sum is over different Feynman diagrams g , and $\mathcal{M}_g(p^l)$ is a polynomial yet to be determined with l -power in momentum. We could further determine the power of momentum is counting mass dimensions. Denote the operator “[.]” for counting the power of momenta in the numerator (abbreviated for “PMN” in the following context) for a given quantity. We then implement these operators on equation (2.40), which in turn gives us

$$[\mathcal{A}_n^{\text{YM}}] = [\epsilon_1 \cdot f_{\alpha_1} \cdots f_{\alpha_{r-2}} \cdot \epsilon_n] + [\mathcal{A}_n^{\text{YM}+\phi^3}(\{\bar{\alpha}\}|1, \alpha, n)]. \quad (\text{A.4})$$

Since the PMN of $\epsilon_1 \cdot f_{\alpha_1} \cdots f_{\alpha_{r-2}} \cdot \epsilon_n$ and $\mathcal{A}_n^{\text{YM}}$ are respectively

$$[\mathcal{A}_n^{\text{YM}}] = n - 2, \quad [\epsilon_1 \cdot f_{\alpha_1} \cdots f_{\alpha_{r-2}} \cdot \epsilon_n] = r - 2, \quad (\text{A.5})$$

then the PMN for the mixed amplitude $\mathcal{A}_n^{\text{YM}+\phi^3}(\{\bar{\alpha}\}|1, \alpha, n)$ is

$$[\mathcal{A}_n^{\text{YM}+\phi^3}(\{\bar{\alpha}\}|1, \alpha, n)] = n - r. \quad (\text{A.6})$$

Based on these analysis, the PMN of our anstaz is confirmed to be $n - r$, thus it becomes

$$M_n(p^{n-r}) = \sum_g \frac{\mathcal{M}_g(p^{n-r})}{\prod_i P_{g,i}}. \quad (\text{A.7})$$

The idea is to show that inserting gluons will not affect the number of minimal basis. Or equivalent saying, if all terms in a r -scalar ϕ^3 amplitude has been given, then no matter inserting how many external gluons, the mixed amplitude $\mathcal{A}_n^{\text{YM}+\phi^3}(\{\bar{\alpha}\}|1, \alpha, n)$ can always be fixed by the r -scalar amplitude $\mathcal{A}_r^{\phi^3}(1, \alpha, n)$. We will use mathematical induction in our proof, in which we admit that at n -point level with r scalars insertion whose $n - r$ gluons satisfy gauge invariance, the mixed amplitude $\mathcal{A}_n^{\text{YM}+\phi^3}(\{\bar{\alpha}\}|1, \alpha, n)$ can be uniquely determined by r -scalar amplitude $\mathcal{A}_r^{\phi^3}$ (or mixed amplitude $\mathcal{A}_3^{\text{YM}+\phi^3}(2|1, 3)$ in case of $r = 2$), and the scalar amplitudes themselves can produce \mathcal{C}_{r-2} minimal basis.

Now we insert a gluon external leg, with its momentum p_{n+1} . Denote

$$p_{n+1}^\mu = zq^\mu. \quad (\text{A.8})$$

There are two possible ways of insertion that is consistent with Feynman rules:

1. If the gluon (denoted as “ q ”) is injected on the λ -th external leg (see fig.19), this corresponds to the singular pole with the propagator $s_{\lambda, n+1} = 2zp_\lambda \cdot q$, while on other propagators, z only contributes to spurious poles such that no singularities occurs.
2. If on the other hand, the gluon is inserted on a propagator between λ -th and $(\lambda+1)$ -th

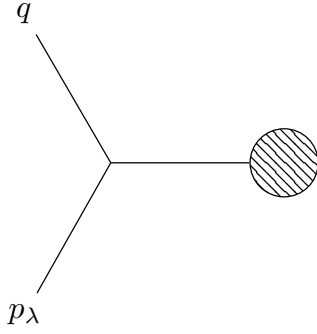


Figure 19: Gluon inserted on an external leg.

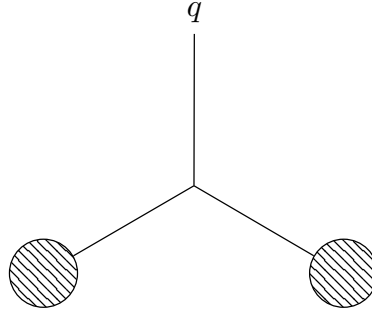


Figure 20: Gluon inserted on a propagator.

external legs (see fig.20), such diagram can be factored out as

$$\frac{N(z)}{P_L(z)(p_1 + \dots + p_\lambda)^2(zq + p_1 + \dots + p_\lambda)^2 P_R(z)}, \quad (\text{A.9})$$

where $P_L(z)$ is the product of propagators on the left of λ -th external leg and $P_R(z)$ denotes the product of propagators on the right of the $(\lambda + 1)$ -th external leg.

Based on these discussions, we can now perform a soft-momentum expansion on our $(n + 1)$ -point ansatz:

$$M_{n+1} = z^{\ell_{\min}} M_{n+1}^{(\ell_{\min})} + z^{\ell_{\min}+1} M_{n+1}^{(\ell_{\min}+1)} \dots + z^{\ell_{\max}} M_{n+1}^{(\ell_{\max})}. \quad (\text{A.10})$$

Note that for the lowest degree ℓ_{\min} , it can be given by one diagram has singular pole with numerator independent of z . This tells us that $\ell_{\min} = -1$. For the highest degree ℓ_{\max} , since we have shown that the PMN of M_{n+1} previously is $n + 1 - r$, then as an extreme, we expect all momenta contribute to it is just q when the propagators are non-singular. This tells us $\ell_{\max} = n + 1 - r$. Thus the soft expansion can be written as

$$M_{n+1} = \frac{M_{n+1}^{(-1)}}{z} + M_{n+1}^{(0)} + z M_{n+1}^{(1)} \dots + z^{n+1-r} M_{n+1}^{(n+1-r)}. \quad (\text{A.11})$$

This indicates that we only need to prove our claim in each expansion order of M_{n+1} . We illustrate our idea in several steps:⁹

At the leading order, we set $(n + 1)$ -th gluon injecting after the n -th particle. By this operation, we obtain a new ordering, say $\text{Tr}(1, 2, \dots, n + 1)$. Note that the ordering obeys the Z_{n+1} symmetry, which indicates that

$$\text{Tr}(1, 2, \dots, n + 1) = \text{Tr}(n + 1, 1, 2, \dots, n). \quad (\text{A.12})$$

⁹Without loss of generality, we assume the color ordering of the $(n + 1)$ -point mixed amplitude to be

$$\mathcal{A}_{n+1}^{\text{YM}+\phi^3}(\underbrace{\{r, r + 1, \dots, n - 1, n + 1\}}_{n+1-r \text{ gluons}} | \underbrace{1, 2, \dots, r - 1, n}_{r \text{ scalars}}) =: \mathcal{A}_{n+1}^{\text{YM}+\phi^3}(r).$$

This shows us that inserting a gluon after the n -th particle is equivalent to insert it before the first particle, revealing that $M_{n+1}^{(-1)}$ has two singular poles

$$M_{n+1}^{(-1)}(p^{n+1-r}) = \frac{\epsilon_{n+1}^\mu \Gamma_\mu(p^{n+1-r})}{q \cdot p_1} + \frac{\epsilon_{n+1}^\mu \Delta_\mu(p^{n+1-r})}{q \cdot p_n}. \quad (\text{A.13})$$

Gauge invariance at $(n+1)$ -th gluon requires that both $\Gamma_\mu(p^{n+1-r})$ and $\Delta_\mu(p^{n+1-r})$ can be factored out as

$$\Gamma_\mu(p^{n+1-r}) = (p_1)_\mu \Gamma(p^{n-r}), \quad \Delta_\mu(p^{n+1-r}) = -(p_n)_\mu \Gamma(p^{n-r}), \quad (\text{A.14})$$

where $\Gamma(p^{n-r})$ is an arbitrary ansatz in terms of (A.7). This leads to

$$M_{n+1}^{(-1)}(p^{n+1-r}) = \left(\frac{\epsilon_{n+1} \cdot p_1}{q \cdot p_1} - \frac{\epsilon_{n+1} \cdot p_n}{q \cdot p_n} \right) \Gamma(p^{n-r}). \quad (\text{A.15})$$

Note that since $\Gamma(p^{n-r})$ is gauge invariant in $n-r$ gluons, by our induction assumption, such ansatz can be fixed with $\mathcal{A}_n^{\text{YM}+\phi^3}(r)$. In this way, we find that the leading order $M_{n+1}^{(-1)}$ is given by the leading order of $\mathcal{A}_{n+1}^{\text{YM}+\phi^3}(r)$, *i.e.*

$$M_{n+1}^{(-1)}(p^{n+1-r}) = \left[\mathcal{A}_{n+1}^{\text{YM}+\phi^3}(r) \right]^{(-1)}. \quad (\text{A.16})$$

At the sub-leading order, there are two types of denominator now: either linear in q or being a polynomial of q . This gives us two types of terms in the following:

$$M_{n+1}^{(0)}(p^{n+1-r}) = \sum_{i=1,n} \frac{\epsilon_{n+1}^\mu q^\nu \Gamma_{i;\mu\nu}(p^{n-r})}{q \cdot p_i} + \sum_{i=2}^{n-1} \frac{\epsilon_{n+1}^\mu \Delta_{i;\mu}(p^{n-r+1})}{P_i}, \quad (\text{A.17})$$

where $P_i := (p_1 + \dots + p_i)^2$. Note that since $\Delta_{i;\mu}(p^{n+1-r})$ is lack of the polarization vector, it can not achieve gauge invariance for $n-r+1$ gluons. However at the same time, it is required that $M_{n+1}^{(0)}(p^{n+1-r})$ should be gauge invariant in these gluons, hence the only choice left for $\Delta_{i;\mu}(p^{n+1-r})$ is to vanish. For terms associated with the singular poles, one can let

$$\Gamma_{n;\mu\nu}(p^{n-r}) = -\frac{q \cdot p_n}{q \cdot p_1} \Gamma_{1;\mu\nu}(p^{n-r}) \quad (\text{A.18})$$

to anti-symmetrize the prefactor in (A.17):

$$M_{n+1}^{(0)}(p^{n+1-r}) = \epsilon_{n+1}^{[\mu} q^{\nu]} \Gamma_{1;\mu\nu}(p^{n-r}). \quad (\text{A.19})$$

Thus alike the case in the leading order term, $\Gamma_{1;\mu\nu}(p^{n-r})$ has maximally $n-r$ $\epsilon \cdot p$ terms and gauged in $n-r$ gluons, which can be again fixed by $\mathcal{A}_n^{\text{YM}+\phi^3}(r)$. For this reason, we conclude that

$$M_{n+1}^{(0)}(p^{n+1-r}) = \left[\mathcal{A}_{n+1}^{\text{YM}+\phi^3}(r) \right]^{(0)}. \quad (\text{A.20})$$

At the sub-sub-leading order, analogously we have

$$M_{n+1}^{(1)}(p^{n+1-r}) = \epsilon_{n+1}^{[\mu} q^{\nu]} \sum_{i=1, n} \frac{q^\rho \Gamma_{i; \mu\nu\rho}(p^{n-1-r})}{q \cdot p_i} + \sum_{i=2}^{n-1} \frac{\Delta_{i; \mu\nu}(p^{n-r})}{P_i}. \quad (\text{A.21})$$

For the first terms $\Gamma_{i; \mu\nu\rho}(p^{n-1-r})$, we require it to be gauge invariant in $n-r$ gluons, whereas the PMN of it is only $n-r-1$. [54] has shown that such terms should be ruled out under this condition, then only the second terms survive in this manner

$$M_{n+1}^{(1)}(p^{n+1-r}) = \epsilon_{n+1}^{[\mu} q^{\nu]} \sum_{i=2}^{n-1} \frac{\Delta_{i; \mu\nu}(p^{n-r})}{P_i}. \quad (\text{A.22})$$

It is obvious that this equation shares the same pattern with our discussion for the sub-leading terms, thus similarly, we obtain

$$M_{n+1}^{(1)}(p^{n+1-r}) = \left[\mathcal{A}_{n+1}^{\text{YM}+\phi^3}(r) \right]^{(1)}. \quad (\text{A.23})$$

At the sub $^{s \geq 3}$ -leading order, it is not straightforward to argue directly that $M_{n+1}^{(s-1)}(p^{n-r+1}) = \left[\mathcal{A}_{n+1}^{\text{YM}+\phi^3}(r) \right]^{(s-1)}$. Instead, we define

$$B_{n+1}^{(s-1)}(p^{n-r+1}) := M_{n+1}^{(s-1)}(p^{n-r+1}) - \left[\mathcal{A}_{n+1}^{\text{YM}+\phi^3}(r) \right]^{(s-1)}, \quad (\text{A.24})$$

and an alternative way is to show that $B_{n+1}^{(s-1)}(p^{n-r+1}) = 0$ for $s \geq 3$. Similarly, $B_{n+1}^{(s-1)}(p^{n-r+1})$ has an expansion of

$$B_{n+1}^{(s-1)}(p^{n-r+1}) = \epsilon_{n+1}^{[\mu} q^{\nu_1]} q^{\nu_2} \dots q^{\nu_s} \left(\sum_{i=1, n} \frac{q^{\nu_{s+1}} \Gamma_{i; \mu\nu_1 \dots \nu_{s+1}}(p^{n-r-s+1})}{q \cdot p_i} + \sum_{i=2}^{n-1} \frac{\Delta_{i; \mu\nu_1 \dots \nu_s}(p^{n-r-s+2})}{P_i} \right). \quad (\text{A.25})$$

Since the PMN of $\Delta_{i; \mu\nu_1 \dots \nu_s}(p^{n-r-s+2})$ is less than $n-r$, there is no space for this factor to be gauge invariant in $n-r$ gluons, which leads to its nullification. Same goes with $\Gamma_{i; \mu\nu_1 \dots \nu_{s+1}}(p^{n-r-s+1})$. Therefore we obtain that $B_{n+1}^{(s-1)}(p^{n-r+1}) = 0$, which tells us that

$$M_{n+1}^{(s-1)}(p^{n-r+1}) = \left[\mathcal{A}_{n+1}^{\text{YM}+\phi^3}(r) \right] \quad \text{for } s \geq 3. \quad (\text{A.26})$$

Summarizing all these discussions, we show that for all order soft expansion, our ansatz can always be fixed by the $(n+1)$ -point mixed amplitude:

$$M_{n+1}(p^{n-r+1}) = \mathcal{A}_{n+1}^{\text{YM}+\phi^3}(r). \quad (\text{A.27})$$

Such relation allows us to induct all the way down to the pure scalar amplitude $\mathcal{A}_r^{\phi^3}$. And for an r -scalar amplitude, it has \mathcal{C}_{r-2} independent basis. This ends our proof.

B Details for 5-point planar universal expansion

The 5-point universal expansion reads:

$$\begin{aligned}
\mathcal{A}_5^{\text{YM}} &= \epsilon_1 \cdot \epsilon_5 \mathcal{A}_5^{\text{YM}+\phi^3}(\{2, 3, 4\} | 1, 5) - \epsilon_1 \cdot f_2 \cdot \epsilon_5 \mathcal{A}_5^{\text{YM}+\phi^3}(\{3, 4\} | 1, 2, 5) \\
&\quad - \epsilon_1 \cdot f_3 \cdot \epsilon_5 \mathcal{A}_5^{\text{YM}+\phi^3}(\{2, 4\} | 1, 3, 5) - \epsilon_1 \cdot f_4 \cdot \epsilon_5 \mathcal{A}_5^{\text{YM}+\phi^3}(\{2, 3\} | 1, 4, 5) \\
&\quad + \epsilon_1 \cdot f_2 \cdot f_3 \cdot \epsilon_5 \mathcal{A}_5^{\text{YM}+\phi^3}(\{4\} | 1, 2, 3, 5) + \epsilon_1 \cdot f_3 \cdot f_2 \cdot \epsilon_5 \mathcal{A}_5^{\text{YM}+\phi^3}(\{4\} | 1, 3, 2, 5) \\
&\quad + \epsilon_1 \cdot f_2 \cdot f_4 \cdot \epsilon_5 \mathcal{A}_5^{\text{YM}+\phi^3}(\{3\} | 1, 2, 4, 5) + \epsilon_1 \cdot f_4 \cdot f_2 \cdot \epsilon_5 \mathcal{A}_5^{\text{YM}+\phi^3}(\{3\} | 1, 4, 2, 5) \\
&\quad + \epsilon_1 \cdot f_3 \cdot f_4 \cdot \epsilon_5 \mathcal{A}_5^{\text{YM}+\phi^3}(\{2\} | 1, 3, 4, 5) + \epsilon_1 \cdot f_4 \cdot f_3 \cdot \epsilon_5 \mathcal{A}_5^{\text{YM}+\phi^3}(\{2\} | 1, 4, 3, 5) \\
&\quad - \epsilon_1 \cdot f_2 \cdot f_3 \cdot f_4 \cdot \epsilon_5 \mathcal{A}_5^{\text{YM}+\phi^3}(\emptyset | 1, 2, 3, 4, 5) - \epsilon_1 \cdot f_2 \cdot f_4 \cdot f_3 \cdot \epsilon_5 \mathcal{A}_5^{\text{YM}+\phi^3}(\emptyset | 1, 2, 4, 3, 5) \\
&\quad - \epsilon_1 \cdot f_3 \cdot f_2 \cdot f_4 \cdot \epsilon_5 \mathcal{A}_5^{\text{YM}+\phi^3}(\emptyset | 1, 3, 2, 4, 5) - \epsilon_1 \cdot f_3 \cdot f_4 \cdot f_2 \cdot \epsilon_5 \mathcal{A}_5^{\text{YM}+\phi^3}(\emptyset | 1, 3, 4, 2, 5) \\
&\quad - \epsilon_1 \cdot f_4 \cdot f_2 \cdot f_3 \cdot \epsilon_5 \mathcal{A}_5^{\text{YM}+\phi^3}(\emptyset | 1, 4, 2, 3, 5) - \epsilon_1 \cdot f_4 \cdot f_3 \cdot f_2 \cdot \epsilon_5 \mathcal{A}_5^{\text{YM}+\phi^3}(\emptyset | 1, 4, 3, 2, 5),
\end{aligned} \tag{B.1}$$

According to (6.1) the original amplitudes are reorganized into:

$$\mathcal{A}_5^{\text{YM}+\phi^3}(\{2, 3, 4\} | 1, 5) = \mathbf{A}_5^{\text{YM}+\phi^3}(\{2, 3, 4\} | 15), \tag{B.2}$$

$$\mathcal{A}_5^{\text{YM}+\phi^3}(\{3, 4\} | 1, 2, 5) = \mathbf{A}_5^{\text{YM}+\phi^3}(\{3, 4\} | 125), \tag{B.3}$$

$$\mathcal{A}_5^{\text{YM}+\phi^3}(\{2, 4\} | 1, 3, 5) = \mathbf{A}_5^{\text{YM}+\phi^3}(\{2, 4\} | 135), \tag{B.4}$$

$$\mathcal{A}_5^{\text{YM}+\phi^3}(\{2, 3\} | 1, 4, 5) = \mathbf{A}_5^{\text{YM}+\phi^3}(\{2, 3\} | 145), \tag{B.5}$$

$$\mathcal{A}_5^{\text{YM}+\phi^3}(\{4\} | 1, 2, 3, 5) = \mathbf{A}_5^{\text{YM}+\phi^3}(\{4\} | 1235) + \mathbf{A}_5^{\text{YM}+\phi^3}(\{4\} | 1[23]5), \tag{B.6}$$

$$\mathcal{A}_5^{\text{YM}+\phi^3}(\{4\} | 1, 3, 2, 5) = -\mathbf{A}_5^{\text{YM}+\phi^3}(\{4\} | 1[23]5), \tag{B.7}$$

$$\mathcal{A}_5^{\text{YM}+\phi^3}(\{3\} | 1, 2, 4, 5) = \mathbf{A}_5^{\text{YM}+\phi^3}(\{3\} | 1245) + \mathbf{A}_5^{\text{YM}+\phi^3}(\{3\} | 1[24]5), \tag{B.8}$$

$$\mathcal{A}_5^{\text{YM}+\phi^3}(\{3\} | 1, 4, 2, 5) = -\mathbf{A}_5^{\text{YM}+\phi^3}(\{3\} | 1[24]5), \tag{B.9}$$

$$\mathcal{A}_5^{\text{YM}+\phi^3}(\{2\} | 1, 3, 4, 5) = \mathbf{A}_5^{\text{YM}+\phi^3}(\{2\} | 1345) + \mathbf{A}_5^{\text{YM}+\phi^3}(\{2\} | 1[34]5), \tag{B.10}$$

$$\mathcal{A}_5^{\text{YM}+\phi^3}(\{2\} | 1, 4, 3, 5) = -\mathbf{A}_5^{\text{YM}+\phi^3}(\{2\} | 1[34]5), \tag{B.11}$$

$$\mathcal{A}_5^{\text{YM}+\phi^3}(\emptyset | 1, 2, 3, 4, 5) = \mathbf{A}_5^{\text{YM}+\phi^3}(\emptyset | 12345) + \mathbf{A}_5^{\text{YM}+\phi^3}(\emptyset | 1[[23]4]5) \tag{B.12}$$

$$+ \mathbf{A}_5^{\text{YM}+\phi^3}(\emptyset | 12[34]5) + \mathbf{A}_5^{\text{YM}+\phi^3}(\emptyset | 1[23]45) \tag{B.13}$$

$$+ \mathbf{A}_5^{\text{YM}+\phi^3}(\emptyset | 1[2[34]5]), \tag{B.14}$$

$$\mathcal{A}_5^{\text{YM}+\phi^3}(\emptyset | 1, 2, 4, 3, 5) = -\mathbf{A}_5^{\text{YM}+\phi^3}(\emptyset | 12[34]5) - \mathbf{A}_5^{\text{YM}+\phi^3}(\emptyset | 1[2[34]5]), \tag{B.15}$$

$$\mathcal{A}_5^{\text{YM}+\phi^3}(\emptyset | 1, 3, 2, 4, 5) = -\mathbf{A}_5^{\text{YM}+\phi^3}(\emptyset | 1[23]45) - \mathbf{A}_5^{\text{YM}+\phi^3}(\emptyset | 1[[23]4]5), \tag{B.16}$$

$$\mathcal{A}_5^{\text{YM}+\phi^3}(\emptyset | 1, 3, 4, 2, 5) = \mathbf{A}_5^{\text{YM}+\phi^3}(\emptyset | 1[2[34]5]), \tag{B.17}$$

$$\mathcal{A}_5^{\text{YM}+\phi^3}(\emptyset | 1, 4, 2, 3, 5) = \mathbf{A}_5^{\text{YM}+\phi^3}(\emptyset | 1[[23]4]5), \tag{B.18}$$

$$\mathcal{A}_5^{\text{YM}+\phi^3}(\emptyset | 1, 4, 3, 2, 5) = -\mathbf{A}_5^{\text{YM}+\phi^3}(\emptyset | 1[[23]4]5) - \mathbf{A}_5^{\text{YM}+\phi^3}(\emptyset | 1[2[34]5]), \tag{B.19}$$

which leads to (6.10).

Bibliography

- [1] Z. Bern, J.J.M. Carrasco and H. Johansson, *New Relations for Gauge-Theory Amplitudes*, *Phys. Rev. D* **78** (2008) 085011 [[0805.3993](#)].
- [2] Z. Bern, J.J.M. Carrasco and H. Johansson, *Perturbative Quantum Gravity as a Double Copy of Gauge Theory*, *Phys. Rev. Lett.* **105** (2010) 061602 [[1004.0476](#)].
- [3] F. Cachazo, S. He and E.Y. Yuan, *Scattering equations and Kawai-Lewellen-Tye orthogonality*, *Phys. Rev. D* **90** (2014) 065001 [[1306.6575](#)].
- [4] F. Cachazo, S. He and E.Y. Yuan, *Scattering of Massless Particles in Arbitrary Dimensions*, *Phys. Rev. Lett.* **113** (2014) 171601 [[1307.2199](#)].
- [5] F. Cachazo, S. He and E.Y. Yuan, *Scattering of Massless Particles: Scalars, Gluons and Gravitons*, *JHEP* **07** (2014) 033 [[1309.0885](#)].
- [6] C.R. Mafra, O. Schlotterer and S. Stieberger, *Explicit BCJ Numerators from Pure Spinors*, *JHEP* **07** (2011) 092 [[1104.5224](#)].
- [7] C.-H. Fu, Y.-J. Du, R. Huang and B. Feng, *Expansion of Einstein-Yang-Mills Amplitude*, *JHEP* **09** (2017) 021 [[1702.08158](#)].
- [8] Y.-J. Du and F. Teng, *BCJ numerators from reduced Pfaffian*, *JHEP* **04** (2017) 033 [[1703.05717](#)].
- [9] F. Teng and B. Feng, *Expanding Einstein-Yang-Mills by Yang-Mills in CHY frame*, *JHEP* **05** (2017) 075 [[1703.01269](#)].
- [10] C. Cheung and Z. Moss, *Symmetry and Unification from Soft Theorems and Unitarity*, *JHEP* **05** (2021) 161 [[2012.13076](#)].
- [11] A. Edison and F. Teng, *Efficient Calculation of Crossing Symmetric BCJ Tree Numerators*, *JHEP* **12** (2020) 138 [[2005.03638](#)].
- [12] S. He, L. Hou, J. Tian and Y. Zhang, *Kinematic numerators from the worldsheet: cubic trees from labelled trees*, *JHEP* **08** (2021) 118 [[2103.15810](#)].
- [13] F.-S. Wei and K. Zhou, *Expanding single-trace YMS amplitudes with gauge-invariant coefficients*, *Eur. Phys. J. C* **84** (2024) 29 [[2306.14774](#)].
- [14] G. Chen, L. Rodina and C. Wen, *Kinematic Hopf algebra and Bern-Carrasco-Johansson numerators at finite α'* , *Phys. Rev. D* **110** (2024) L041902 [[2403.04614](#)].
- [15] H. Gomez, *A Novel On-Shell Recursive Relation*, [2507.23510](#).
- [16] V. Del Duca, L.J. Dixon and F. Maltoni, *New color decompositions for gauge amplitudes at tree and loop level*, *Nucl. Phys. B* **571** (2000) 51 [[hep-ph/9910563](#)].
- [17] N. Arkani-Hamed, H. Frost, G. Salvatori, P.-G. Plamondon and H. Thomas, *All Loop Scattering as a Counting Problem*, [2309.15913](#).
- [18] N. Arkani-Hamed, H. Frost, G. Salvatori, P.-G. Plamondon and H. Thomas, *All Loop Scattering For All Multiplicity*, [2311.09284](#).
- [19] N. Arkani-Hamed, Q. Cao, J. Dong, C. Figueiredo and S. He, *Hidden zeros for particle/string amplitudes and the unity of colored scalars, pions and gluons*, *JHEP* **10** (2024) 231 [[2312.16282](#)].
- [20] N. Arkani-Hamed, Q. Cao, J. Dong, C. Figueiredo and S. He, *Scalar-scaffolded gluons and the combinatorial origins of Yang-Mills theory*, *JHEP* **04** (2025) 078 [[2401.00041](#)].

- [21] N. Arkani-Hamed, Q. Cao, J. Dong, C. Figueiredo and S. He, *Nonlinear Sigma model amplitudes to all loop orders are contained in the $Tr(\Phi^3)$ theory*, *Phys. Rev. D* **110** (2024) 065018 [[2401.05483](#)].
- [22] Q. Cao, J. Dong, S. He and C. Shi, *A universal splitting of string and particle scattering amplitudes*, [2403.08855](#).
- [23] C. Bartsch, T.V. Brown, K. Kampf, U. Oktem, S. Paranjape and J. Trnka, *Hidden Amplitude Zeros From Double Copy*, [2403.10594](#).
- [24] Y. Li, D. Roest and T. ter Veldhuis, *Hidden Zeros in Scaffolded General Relativity and Exceptional Field Theories*, [2403.12939](#).
- [25] N. Arkani-Hamed and C. Figueiredo, *All-order splits and multi-soft limits for particle and string amplitudes*, [2405.09608](#).
- [26] L. Rodina, *Hidden Zeros Are Equivalent to Enhanced Ultraviolet Scaling, and Lead to Unique Amplitudes in $Tr(\phi^3)$ Theory*, *Phys. Rev. Lett.* **134** (2025) 031601 [[2406.04234](#)].
- [27] Q. Cao, J. Dong, S. He, C. Shi and F. Zhu, *On universal splittings of tree-level particle and string scattering amplitudes*, [2406.03838](#).
- [28] K. Zhou, *Understanding zeros and splittings of ordered tree amplitudes via Feynman diagrams*, *JHEP* **03** (2025) 154 [[2411.07944](#)].
- [29] Y. Li, T. Wang, T. Brauner and D. Roest, *Diagrammatic Derivation of Hidden Zeros and Exact Factorization of Pion Scattering Amplitudes*, *Phys. Rev. Lett.* **135** (2025) 181601 [[2412.14858](#)].
- [30] B. Giménez Umbert and K. Yeats, *ϕp amplitudes from the positive tropical Grassmannian: Triangulations of extended diagrams*, *Phys. Rev. D* **110** (2024) 125018 [[2403.17051](#)].
- [31] Y. Zhang, *On the new factorizations of Yang-Mills amplitudes*, *JHEP* **02** (2025) 074 [[2412.15198](#)].
- [32] Y. Zhang, *New factorizations of Yang-Mills amplitudes*, *Phys. Rev. D* **111** (2025) 085004 [[2406.08969](#)].
- [33] S. De, S. Paranjape, A. Pokraka, M. Spradlin and A. Volovich, *Hidden zeros of the cosmological wavefunction*, *JHEP* **07** (2025) 174 [[2503.23579](#)].
- [34] J.V. Backus and L. Rodina, *Emergence of Unitarity and Locality from Hidden Zeros at One-Loop Order*, *Phys. Rev. Lett.* **135** (2025) 131601 [[2503.03805](#)].
- [35] Y.-C. Chang, H.-Y. Chen and Y.-t. Huang, *All zeros of (super)String Theory*, [2506.15299](#).
- [36] B. Feng, L. Zhang and K. Zhou, *Hidden zeros and 2-split via BCFW recursion relation*, *JHEP* **08** (2025) 205 [[2504.14215](#)].
- [37] B. Feng, L. Zhang and K. Zhou, *2-split from Feynman diagrams and Expansions*, [2508.21345](#).
- [38] L. Zhang, *2-Split of Form Factors via BCFW Recursion Relation*, [2509.12564](#).
- [39] K. Zhou, *Hidden zeros for higher-derivative YM and GR amplitudes at tree-level*, [2510.11070](#).
- [40] C. Cheung, C.-H. Shen and C. Wen, *Unifying Relations for Scattering Amplitudes*, *JHEP* **02** (2018) 095 [[1705.03025](#)].

- [41] J.V. Backus and C. Figueiredo, *Surface gauge invariance, soft limits and the transmutation of gluons into scalars*, *JHEP* **09** (2025) 069 [2505.17179].
- [42] N. Arkani-Hamed, Q. Cao, J. Dong, C. Figueiredo and S. He, *Surface Kinematics and the Canonical Yang-Mills All-Loop Integrand*, *Phys. Rev. Lett.* **134** (2025) 171601 [2408.11891].
- [43] N. Arkani-Hamed, F. Cachazo and J. Kaplan, *What is the Simplest Quantum Field Theory?*, *JHEP* **09** (2010) 016 [0808.1446].
- [44] S. Stieberger and T.R. Taylor, *Graviton as a Pair of Collinear Gauge Bosons*, *Phys. Lett. B* **739** (2014) 457 [1409.4771].
- [45] S. Stieberger and T.R. Taylor, *Graviton Amplitudes from Collinear Limits of Gauge Amplitudes*, *Phys. Lett. B* **744** (2015) 160 [1502.00655].
- [46] F. Cachazo, S. He and E.Y. Yuan, *New Double Soft Emission Theorems*, *Phys. Rev. D* **92** (2015) 065030 [1503.04816].
- [47] N. Arkani-Hamed, Y. Bai, S. He and G. Yan, *Scattering Forms and the Positive Geometry of Kinematics, Color and the Worldsheet*, *JHEP* **05** (2018) 096 [1711.09102].
- [48] F. Cachazo, S. He and E.Y. Yuan, *Scattering Equations and Matrices: From Einstein To Yang-Mills, DBI and NLSM*, *JHEP* **07** (2015) 149 [1412.3479].
- [49] C. Cheung, G.N. Remmen, C.-H. Shen and C. Wen, *Pions as Gluons in Higher Dimensions*, *JHEP* **04** (2018) 129 [1709.04932].
- [50] C.S. Lam and Y.-P. Yao, *Evaluation of the Cachazo-He-Yuan gauge amplitude*, *Phys. Rev. D* **93** (2016) 105008 [1602.06419].
- [51] J. Dong, S. He and L. Hou, *Universal expansions of scattering amplitudes for gravitons, gluons, and Goldstone particles*, *Phys. Rev. D* **105** (2022) 105007 [2111.10525].
- [52] N. Arkani-Hamed, L. Rodina and J. Trnka, *Locality and Unitarity of Scattering Amplitudes from Singularities and Gauge Invariance*, *Phys. Rev. Lett.* **120** (2018) 231602 [1612.02797].
- [53] R. Kleiss and H. Kuijf, *Multi - Gluon Cross-sections and Five Jet Production at Hadron Colliders*, *Nucl. Phys. B* **312** (1989) 616.
- [54] L. Rodina, *Uniqueness from gauge invariance and the Adler zero*, *JHEP* **09** (2019) 084 [1612.06342].
- [55] Z. Bern and T. Dennen, *A Color Dual Form for Gauge-Theory Amplitudes*, *Phys. Rev. Lett.* **107** (2011) 081601 [1103.0312].
- [56] Q. Cao, J. Dong, S. He and F. Zhu, *Superstring amplitudes meet surfaceology*, 2504.21676.
- [57] J.V. Backus, *New Recursions for the Canonical Scalar-Scaffolded Yang-Mills Amplitude*, 2510.19901.
- [58] S. De, A. Pokraka, M. Skowronek, M. Spradlin and A. Volovich, *Surfaceology for colored Yukawa theory*, *JHEP* **09** (2024) 160 [2406.04411].
- [59] N. Arkani-Hamed, C. Figueiredo, H. Frost and G. Salvatori, *Tropical Amplitudes For Colored Lagrangians*, 2402.06719.
- [60] F.M. Balli, A. Edison and O. Schlotterer, *Pinching rules in the chiral-splitting description of one-loop string amplitudes*, *JHEP* **05** (2025) 101 [2410.19641].
- [61] Y. Geyer, J. Guo, R. Monteiro and L. Ren, *Superstring amplitudes from BCJ numerators at one loop*, *JHEP* **03** (2025) 017 [2410.19663].

- [62] Q. Cao, J. Dong, S. He and F. Zhu, *One-loop amplitudes in gauge theories*, *Phys. Rev. D* **111** (2025) 065015 [[2412.19629](#)].
- [63] Q. Cao, S. He, Y. Zhang and F. Zhu, *Loop-Level Double Copy Relations from Forward Limits*, [2509.25129](#).
- [64] R. Monteiro and L. Ren, *Superstring amplitudes from the field-theory limit: an n-point map at one loop*, [2510.02455](#).
- [65] Y.-J. Du, C.-H. Fu, Y. Wang and C. Xie, *Algebraic Consistency and Explicit Construction of One-Loop BCJ Numerators of Yang-Mills and Related Theories*, [2511.10963](#).